

Syddansk Universitet

Microbial methanogenesis in the sulfate-reducing zone in sediments from Eckernförde Bay, SW Baltic Sea

Maltby, Johanna ; Steinle, Lea; Löscher, Carolin; Bange, Hermann W; Fischer, Martin ; Treude, Tina; Schmidt, Markus

Published in:
Biogeosciences Discussions

Publication date:
2017

Document version
Peer reviewed version

Document license
CC BY

Citation for pulished version (APA):
Maltby, J., Steinle, L., Löscher, C., Bange, H. W., Fischer, M., Treude, T., & Schmidt, M. (2017). Microbial methanogenesis in the sulfate-reducing zone in sediments from Eckernförde Bay, SW Baltic Sea. Biogeosciences Discussions.

General rights

Copyright and moral rights for the publications made accessible in the public portal are retained by the authors and/or other copyright owners and it is a condition of accessing publications that users recognise and abide by the legal requirements associated with these rights.

- Users may download and print one copy of any publication from the public portal for the purpose of private study or research.
- You may not further distribute the material or use it for any profit-making activity or commercial gain
- You may freely distribute the URL identifying the publication in the public portal ?

Take down policy

If you believe that this document breaches copyright please contact us providing details, and we will remove access to the work immediately and investigate your claim.



25 Abstract

26 The presence of surface methanogenesis, located within the sulfate-reducing zone (0-30 centimeters
 27 below seafloor, cmbsf), was investigated in sediments of the seasonally hypoxic Eckernförde Bay,
 28 southwestern Baltic Sea. Water column parameters like oxygen, temperature and salinity together
 29 with porewater geochemistry and benthic methanogenesis rates were determined in the sampling
 30 area “Boknis Eck” quarterly from March 2013 to September 2014, to investigate the effect of
 31 seasonal environmental changes on the rate and distribution of surface methanogenesis and to
 32 estimate its potential contribution to benthic methane emissions. The metabolic pathway of
 33 methanogenesis in the presence or absence of sulfate reducers and after the addition of a non-
 34 competitive substrate was studied in four experimental setups: 1) unaltered sediment batch
 35 incubations (net methanogenesis), 2) ^{14}C -bicarbonate labeling experiments (hydrogenotrophic
 36 methanogenesis), 3) manipulated experiments with addition of either molybdate (sulfate reducer
 37 inhibitor), 2-bromoethane-sulfonate (methanogen inhibitor), or methanol (non-competitive
 38 substrate, potential methanogenesis), 4) addition of ^{13}C -labeled methanol (potential methylotrophic
 39 methanogenesis). After incubation with methanol in the manipulated experiments, molecular
 40 analyses were conducted to identify key functional methanogenic groups. Hydrogenotrophic
 41 methanogenesis in sediments below the sulfate-reducing zone (> 30 cmbsf) was determined by ^{14}C -
 42 bicarbonate radiotracer incubation in samples collected in September 2013.

43 Surface methanogenesis changed seasonally in the upper 30 cmbsf with rates increasing from March
 44 ($0.2 \text{ nmol cm}^{-3} \text{ d}^{-1}$) to November ($1.3 \text{ nmol cm}^{-3} \text{ d}^{-1}$) 2013 and March ($0.2 \text{ nmol cm}^{-3} \text{ d}^{-1}$) to September
 45 ($0.4 \text{ nmol cm}^{-3} \text{ d}^{-1}$) 2014, respectively. Its magnitude and distribution appeared to be controlled by
 46 organic matter availability, C/N, temperature, and oxygen in the water column, revealing higher rates
 47 in warm, stratified, hypoxic seasons (September/November) compared to colder, oxygenated
 48 seasons (March/June) of each year. The majority of surface methanogenesis was likely driven by the
 49 usage of non-competitive substrates (e.g., methanol and methylated compounds), to avoid
 50 competition with sulfate reducers, as it was indicated by the 1000-3000-fold increase in potential
 51 methanogenesis activity observed after methanol addition. Accordingly, competitive
 52 hydrogenotrophic methanogenesis increased in the sediment only below the depth of sulfate
 53 penetration (> 30 cmbsf). Members of the family *Methanosarcinaceae*, which are known for
 54 methylotrophic methanogenesis, were detected by PCR using *Methanosarcinaceae*-specific primers
 55 and are likely to be responsible for the observed surface methanogenesis.

56 The present study indicated that surface methanogenesis makes an important contribute to the
 57 benthic methane budget of Eckernförde Bay sediments as it could directly feed into methane
 58 oxidation above the sulfate-methane transition zone.



59 1. Introduction

60 After water vapor and carbon dioxide, methane is the most abundant greenhouse gas in the
61 atmosphere (e.g. Hartmann et al., 2013; Denman et al., 2007). Its atmospheric concentration
62 increased more than 150 % since preindustrial times, mainly through increased human activities such
63 as fossil fuel usage and livestock breeding (Hartmann et al., 2013; Wuebbles & Hayhoe, 2002;
64 Denman et al., 2007). Determining the natural and anthropogenic sources of methane is one of the
65 major goals for oceanic, terrestrial and atmospheric scientists to be able to predict further impacts
66 on the world's climate. The ocean is considered to be a modest natural source for atmospheric
67 methane (Wuebbles & Hayhoe, 2002; Reeburgh, 2007; EPA, 2010). However, research is still sparse
68 on the origin of the observed oceanic methane, which automatically leads to uncertainties in current
69 ocean flux estimations (Bange et al., 1994; Naqvi et al., 2010; Bakker et al., 2014).

70 Within the marine environment, the coastal areas (including estuaries and shelf regions) are
71 considered the major source for atmospheric methane, contributing up to 75 % to the global ocean
72 methane production (Bange et al., 1994). The major part of the coastal methane is produced during
73 microbial methanogenesis in the sediment, with probably only a minor part originating from
74 methane production within the water column (Bakker et al., 2014). However, the knowledge on
75 magnitude, seasonality and environmental controls of benthic methanogenesis is still limited.
76 In marine sediments, methanogenesis activity is mostly restricted to the sediment layers below
77 sulfate reduction, due to the successful competition of sulfate reducers with methanogens for the
78 mutual substrates acetate and hydrogen (H_2) (Oremland & Polcin, 1982; Crill & Martens, 1986;
79 Jørgensen, 2006). Methanogens produce methane mainly from using acetate (acetoclastic
80 methanogenesis) or H_2 and carbon dioxide (CO_2) (hydrogenotrophic methanogenesis). Competition
81 with sulfate reducers can be relieved through usage of non-competitive substrates (e.g. methanol or
82 methylated compounds, methylotrophic methanogenesis) (Cicerone & Oremland, 1988; Oremland &
83 Polcin, 1982). Coexistence of sulfate reduction and methanogenesis has been detected in a few
84 studies from organic-rich sediments, e.g., salt-marsh sediments (Oremland et al., 1982; Buckley et al.,
85 2008), coastal sediments (Holmer & Kristensen, 1994; Jørgensen & Parkes, 2010) or sediments in
86 upwelling regions (Pimenov et al., 1993; Ferdelman et al., 1997; Maltby et al., 2016), indicating the
87 importance of these environments for surface methanogenesis. So far, however, environmental
88 control mechanisms of surface methanogenesis remain elusive.

89 The coastal inlet Eckernförde Bay (southwestern Baltic Sea) is an excellent model environment to
90 study seasonal and environmental control mechanisms of benthic surface methanogenesis. Here,
91 the muddy sediments are characterized by high organic loading and high sedimentation rates
92 (Whiticar, 2002), which lead to anoxic conditions within the uppermost 0.1-0.2 centimeter below
93 seafloor (cmbsf) (Preisler et al., 2007). Seasonally hypoxic (dissolved oxygen $< 63 \mu M$) and anoxic



(dissolved oxygen = 0 μM) events in the bottom water of Eckernförde Bay (Lennartz et al., 2014) provide ideal conditions for anaerobic processes at the sediment surface. Sulfate reduction is the dominant pathway of organic carbon degradation in Eckernförde Bay sediments in the upper 30 cmbsf, followed by methanogenesis in deeper sediment layers where sulfate is depleted (> 30 cmbsf) (Whiticar 2002; Treude et al. 2005; Martens et al. 1998). This deep methanogenesis can be intense and often leads to methane oversaturation in the porewater below 50 cm sediment depth, resulting in gas bubble formation (Abegg & Anderson, 1997; Whiticar, 2002; Thießen et al., 2006). Thus, methane is transported from the methanogenic zone (> 30 cmbsf) to the surface sediment by both molecular diffusion and advection via rising gas bubbles (Wever et al., 1998; Treude et al., 2005a). Although upward diffusing methane is mostly retained by anaerobic oxidation of methane (AOM) (Treude et al. 2005), a major part is reaching the sediment-water interface through gas bubble transport (Treude et al. 2005; Jackson et al. 1998), resulting in a supersaturation of the water column with respect to atmospheric methane concentrations (Bange et al., 2010). The Time Series Station "Boknis Eck" in the Eckernförde Bay is a known site of methane emissions into the atmosphere throughout the year due to this supersaturation of the water column (Bange et al., 2010). The source for benthic and water column methane was seen in deep methanogenesis (> 30 cmbsf) below the penetration of sulfate (Whiticar, 2002), however, coexistence of sulfate reduction and methanogenesis has been postulated (Whiticar, 2002; Treude et al., 2005a). Still, the magnitude and environmental controls of surface methanogenesis is poorly understood, even though it may make a measurable contribution to benthic methane emissions given its short diffusion distance to the sediment-water interface (Knittel & Boetius, 2009). Production of methane within the sulfate reduction zone of Eckernförde Bay surface sediments could further explain peaks of methane oxidation observed in top sediment layers, which was previously attributed to methane transported to the surface via rising gas bubbles (Treude et al., 2005a). In the present study, we investigated surface sediment (< 30 cmbsf, on a seasonal basis), deep sediment (> 30 cmbsf, on one occasion), and the water column (on a seasonal basis) at the Time Series Station "Boknis Eck" in Eckernförde Bay, to validate the existence of surface methanogenesis and its potential contribution to benthic methane emissions. Water column parameters like oxygen, temperature, and salinity together with porewater geochemistry and benthic methanogenesis were measured over a course of 2 years. In addition to seasonal rate measurements, inhibition and stimulation experiments, stable isotope probing, and molecular analysis were carried out to find out if surface methanogenesis 1) is controlled by environmental parameters, 2) shows seasonal variability, 3) is based on non-competitive substrates with a special focus on methyilotrophic methanogens.



129 2. Material and Methods

130 2.1 Study site

131 Samples were taken at the Time Series Station "Boknis Eck" (BE, 54°31.15 N, 10°02.18 E;
 132 www.bokniseck.de) located at the entrance of Eckernförde Bay in the southwestern Baltic Sea with a
 133 water depth of about 28 m (map of sampling site can be found in e.g. Hansen et al., (1999)). From
 134 mid of March until mid of September the water column is strongly stratified due to the inflow of
 135 saltier North Sea water and a warmer and fresher surface water (Bange et al., 2011). Organic matter
 136 degradation in the deep layers causes pronounced hypoxia (March-Sept) or even anoxia
 137 (August/September) (Smetacek, 1985; Smetacek et al., 1984). The source of organic material is
 138 phytoplankton blooms, which occur regularly in spring (February-March) and fall (September-
 139 November) and are followed by pronounced sedimentation of organic matter (Bange et al., 2011). To
 140 a lesser extent, phytoplankton blooms and sedimentation are also observed during the summer
 141 months (July/August) (Smetacek et al., 1984). Sediments at BE are generally classified as soft, fine-
 142 grained muds (< 40 µm) with a carbon content of 3 to 5 wt% (Balzer et al., 1986). The bulk of organic
 143 matter in Eckernförde Bay sediments originates from marine plankton and macroalgal sources (Orsi
 144 et al., 1996), and its degradation leads to production of free methane gas (Wever & Fiedler, 1995;
 145 Abegg & Anderson, 1997; Wever et al., 1998). The oxygen penetration depth is limited to the upper
 146 few millimeters when bottom waters are oxic (Preisler et al., 2007). Reducing conditions within the
 147 sulfate reduction zone lead to a dark grey/black sediments color with a strong hydrogen sulfur odor
 148 in the upper meter of the sediment and dark olive-green color the deeper sediment layers (> 1 m)
 149 (Abegg & Anderson, 1997).

150 2.2 Water column and sediment sampling

151 Sampling was done on a seasonal basis during the years of 2013 and 2014. One-Day field trips with
 152 either F.S. Alkor (cruise no. AL410), F.K. Littorina or F.B. Polarfuchs were conducted in March, June,
 153 and September of each year. In 2013, additional sampling was conducted in November. At each
 154 sampling month, water profiles of temperature, salinity, and oxygen concentration (optical sensor,
 155 RINKO III, detection limit= 2 µM) were measured with a CTD (Hydro-Bios). In addition, water samples
 156 for methane concentration measurements were taken at 25 m water depth with a 6-Niskin bottle (4
 157 Liter each) rosette attached to the CTD (Table 1). Complementary samples for water column
 158 chlorophyll were taken at 25 m water depth with the CTD-rosette within the same months during
 159 standardized monthly sampling cruises to Boknis Eck organized by GEOMAR.
 160 Sediment cores were taken with a miniature multicorer (MUC, K.U.M. Kiel), holding 4 core liners
 161 (length= 60 cm, diameter= 10 cm) at once. The cores had an average length of ~ 30 cm and were



stored at 10°C in a cold room (GEOMAR) until further processing (normally within 1-3 days after sampling).

In September 2013, a gravity core was taken in addition to the MUC cores. The gravity core was equipped with an inner plastic bag (polyethylene; diameter: 13 cm). After core recovery (330 cm total length), the polyethylene bag was cut open at 12 different sampling depths resulting in intervals of 30 cm and sampled directly on board for sediment porewater geochemistry (see Sect. 2.4), sediment methane (see Sect. 2.5), sediment solid phase geochemistry (see Sect. 2.6), and microbial rate measurements for hydrogenotrophic methanogenesis as described in section 2.8.

2.3 Water column parameters

At each sampling month, water samples for methane concentration measurements were taken at 25 m water depth in triplicates. Therefore, three 25 ml glass vials were filled bubble free directly after CTD-rosette recovery and closed with butyl rubber stoppers. Samples were killed with saturated mercury chloride solution and stored at room temperature until further treatment.

Concentrations of dissolved methane (CH₄) were determined by headspace gas chromatography as described in Bange et al. (2010). Calibration for CH₄ was done by a two-point calibration with known methane concentrations before the measurement of headspace gas samples, resulting in an error of < 5 %.

Water samples for chlorophyll concentration were taken by transferring the complete water volume (from 25 m water depth) from one water sampler into a 4.5 L Nalgene bottle, from which then approximately 0.7-1 L (depending on the plankton content) were filtrated back in the GEOMAR laboratory using GF/F filter (Whatman, 25 mm diameter, 8 µm pores size). Dissolved chlorophyll a concentrations were determined using the fluorometric method by Welschmeyer (1994) with an error < 10 %.

2.4 Sediment porewater geochemistry

Porewater was extracted from sediment within 24 hours after core retrieval using nitrogen (N₂) pre-flushed rhizons (0.2 µm, Rhizosphere Research Products, Seeburg-Elverfeldt et al., 2005). In MUC cores, rhizons were inserted into the sediment in 2 cm intervals through pre-drilled holes in the core liner. In the gravity core, rhizons were inserted into the sediment in 30 cm intervals directly after retrieval.

Extracted porewater from MUC and gravity cores was immediately analyzed for sulfide using standardized photometric methods (Grasshoff et al., 1999).

Sulfate concentrations were determined using ion chromatography (Methrom 761). Analytical precision was < 1 % based on repeated analysis of IAPSO seawater standards (dilution series) with an



absolute detection limit of 1 μM corresponding to a detection limit of 30 μM for the undiluted sample. For analysis of dissolved inorganic carbon (DIC), 1.8 ml of porewater was transferred into a 2 ml glass vial, fixed with 10 μl saturated HgCl_2 solution and crimp sealed. DIC concentration was determined as CO_2 with a multi N/C 2100 analyzer (Analytik Jena) following the manufacturer's instructions. Therefore, the sample was acidified with phosphoric acid and the outgassing CO_2 was measured. The detection limit was 20 μM with a precision of 2-3 %.

2.5 Sediment methane concentrations

In March 2013, June 2013 and March 2014, one MUC core was sliced in 1 cm intervals until 6 cmbsf, followed by 2 cm intervals until the end of the core. At the other sampling months, the MUC core was sliced in 1 cm intervals until 6 cmbsf, followed by 2 cm intervals until 10 cmbsf and 5 cm intervals until the end of the core. Per sediment depth (in MUC and gravity cores), 2 cm^3 of sediment were transferred into a 10 ml-glass vial containing 5 ml NaOH (2.5 %) for determination of sediment methane concentration per volume of sediment. The vial was quickly closed with a butyl septum, crimp-sealed and shaken thoroughly. The vials were stored upside down at room temperature until measurement via gas chromatography. Therefore, 100 μl of headspace was removed from the gas vials and injected into a Shimadzu gas chromatograph (GC-2014) equipped with a packed Haysep-D column and a flame ionization detector. The column temperature was 80°C and the helium flow was set to 12 ml min^{-1} . CH_4 concentrations were calibrated against CH_4 standards (Scotty gases). The detection limit was 0.1 ppm with a precision of 2 %.

2.6 Sediment solid phase geochemistry

Following the sampling for CH_4 , the same cores described under section 2.5 were used for the determination of the sediment solid phase geochemistry, i.e. porosity, particulate organic carbon (POC) and particulate organic nitrogen (PON). Sediment porosity of each sampled sediment section was determined by the weight difference of 5 cm^3 wet sediment after freeze-drying for 24 hours. Dried sediment samples were then used for analysis of particulate organic carbon (POC) and particulate organic nitrogen (PON) with a Carlo-Erba element analyzer (NA 1500). The detection limit for C and N analysis was < 0.1 dry weight percent (%) with a precision of < 2 %.

2.7 Sediment methanogenesis

2.7.1 Methanogenesis in MUC cores

At each sampling month, three MUC cores were sliced in 1 cm intervals until 6 cmbsf, in 2 cm intervals until 10 cmbsf, and in 5 cm intervals until the bottom of the core. Every sediment layer was



transferred to a separate beaker and quickly homogenized before sub-sampling. The exposure time with air, i.e. oxygen, was kept to a minimum. Sediment layers were then sampled for determination of net methanogenesis (defined as the sum of total methane production and consumption, including all available methanogenic substrates in the sediment), hydrogenotrophic methanogenesis (methanogenesis based on the substrates CO_2/H_2), and potential methanogenesis (methanogenesis at ideal conditions, i.e. no lack of nutrients) as described in the following sections.

Net methanogenesis

Net methanogenesis was determined with sediment slurry experiments by measuring the headspace methane concentration over time. Per sediment layer, triplicates of 5 cm^3 of sediment were transferred into N_2 -flushed sterile glass vials (30 ml) and mixed with 5 ml filtered bottom water. The slurry was repeatedly flushed with N_2 to remove residual methane and to ensure complete anoxia. Slurries were incubated in the dark at in-situ temperature, which varied at each sampling date (Table 1). Headspace samples (0.1 ml) were taken out every 3-4 days over a time period of 4 weeks and analyzed on a Shimadzu GC-2104 gas chromatograph (see Sect. 2.5). Net methanogenesis rates were determined by the linear increase of the methane concentration over time (minimum of 6 time points).

Hydrogenotrophic methanogenesis

To determine hydrogenotrophic methanogenesis, radioactive sodium bicarbonate ($\text{NaH}^{14}\text{CO}_3$) was added to the sediment. Per sediment layer, sediment was sampled in triplicates with glass tubes (5 mL) which were closed with butyl rubber stoppers on both ends according to (Treude et al. 2005). Through the stopper, $\text{NaH}^{14}\text{CO}_3$ (dissolved in water, injection volume 6 μl , activity 222 kBq, specific activity = $1.85\text{--}2.22 \text{ GBq/mmol}$) was injected into each sample and incubated for three days in the dark at in-situ temperature (Table 1). To stop bacterial activity, sediment was transferred into 50 ml glass-vials filled with 20 ml sodium hydroxide (2.5 % w/w), closed quickly with rubber stoppers and shaken thoroughly. Five controls were produced from various sediment depths by injecting the radiotracer directly into the NaOH with sediment. The production of ^{14}C -methane was determined with the slightly modified method by Treude et al., (2005) used for the determination of anaerobic oxidation of methane. The method was identical, except no unlabeled methane was determined by gas chromatography. Instead, DIC values were used to calculate hydrogenotrophic methane production.

Potential methanogenesis in manipulated experiments

To examine the interaction between sulfate reduction and methanogenesis, inhibition and stimulation experiments were carried out. Therefore, every other sediment layer was sampled



263 resulting in the following examined six sediment layers: 0-1 cm, 2-3 cm, 4-5 cm, 6-8 cm, 10-15 cm
264 and 20-25 cm. From each layer, sediment slurries were prepared by mixing 5 ml sediment in a 1:1
265 ratio with adapted artificial seawater medium (salinity 24, Widdel & Bak, 1992) in N₂-flushed, sterile
266 glass vials before further manipulations.
267 In total, four different treatments, each in triplicates, were prepared per depth: 1) with sulfate
268 addition (17 mM), 2) with sulfate (17 mM) and molybdate (22 mM) addition, 3) with sulfate (17 mM)
269 and 2-bromoethane-sulfonate (BES, 60 mM) addition, and 4) with sulfate (17 mM) and methanol (10
270 mM) addition. From here on, the following names are used to describe the different treatments,
271 respectively: 1) control treatment, 2) molybdate treatment, 3) BES treatment, and 4) methanol
272 treatment. Control treatments feature the natural sulfate concentrations occurring in surface
273 sediments of the sampling site. Molybdate was used as an enzymatic inhibitor for sulfate reduction
274 (Oremland & Capone, 1988) and BES was used as an inhibitor for methanogenic archaea (Hoehler et
275 al., 1994). Methanol is a known non-competitive substrate, which is used by methanogens but not by
276 sulfate reducers (Oremland & Polcin, 1982), thus it is suitable to examine non-competitive
277 methanogenesis. Treatments were incubated at the respective in-situ temperature (Table 1) in the
278 dark.

279 ***Potential methylotrophic methanogenesis from methanol using stable isotope probing***

280 One additional experiment was conducted with sediments from September 2014 by adding ¹³C-
281 labelled methanol to investigate the production of ¹³C-labelled methane. Three cores were stored at
282 1°C after the September 2014 cruise until further processing ~ 3.5 months later. The low storage
283 temperature and the fast oxygen consumption in the enclosed supernatant water (i.e., exclusion of
284 bioturbation by macrofauna) led to slowed microbial activity and preserved the sediments for
285 potential methanogenesis measurements.
286 Sediment cores were sliced in 2 cm intervals and the upper 0-2 cmbsf sediment layer of all three
287 cores was combined in a beaker and homogenized. Then, sediment slurries were prepared by mixing
288 5 cm⁻³ of sediment with 5 ml of artificial seawater medium in N₂-flushed, sterile glass vials (30 ml).
289 Then, methanol was added to the slurry with a final concentration of 10 mM (see Sect. 2.7.3), but
290 this time the methanol was enriched with ¹³C-labelled methanol in a ratio of 1:1000 between ¹³C-
291 labelled (99.9 % ¹³C) and non-labelled methanol mostly consisting of ¹²C (manufacturer: Roth). In
292 total, 54 vials were prepared for nine different sampling time points during a total incubation time of
293 37 days. All vials were incubated at 13°C (in situ temperature in September 2014) in the dark. At each
294 sampling point, six vials were stopped: one set of triplicates were used for headspace methane and
295 carbon dioxide determination and a second set of triplicates were used for porewater analysis.
296 Headspace methane and carbon dioxide concentrations (volume 100 µl) were determined on a
297 Shimadzu gas chromatograph (GC-2014) equipped with a packed Haysep-D column a flame ionization



detector and a methanizer. The methanizer (reduced nickel) reduces carbon dioxide with hydrogen to methane at a temperature of 400°C. The column temperature was 80°C and the helium flow was set to 12 ml min⁻¹. Methane concentrations (including reduced CO₂) were calibrated against methane standards (Scotty gases). The detection limit was 0.1 ppm with a precision of 2 %. Analyses of ¹³C/¹²C-ratios of methane and carbon dioxide were conducted after headspace concentration measurements by using a continuous flow combustion gas chromatograph (Trace Ultra, Thermo Scientific), which was coupled to an isotope ratio mass spectrometer (MAT253, Thermo Scientific). The isotope ratios of methane and carbon dioxide given in the common delta-notation (δ ¹³C in permill) are reported relative to Vienna Pee Dee Belemnite (VPDB) standard. Isotope precision was +/- 0.5 ‰, when measuring near the detection limit of 10 ppm. For porewater analysis of methanol concentration and isotope composition, each sediment slurry of the triplicates was transferred into argon-flushed 15 ml centrifuge tubes and centrifuged for 6 minutes at 4500 rpm. Then 1 ml filtered (0.2 µm) porewater was transferred into N₂-flushed 2 ml glass vials for methanol analysis, crimp sealed and immediately frozen at -20 °C. Methanol concentrations and isotope composition were determined via high performance liquid chromatography-ion ratio mass spectrometry (HPLC-IRMS, Thermo Fisher Scientific) at the MPI Marburg. The detection limit was 50 µM with a precision of 0.3‰.

2.7.2 Methanogenesis in the gravity core

Ex situ hydrogenotrophic methanogenesis was determined in a gravity core taken September 2013. The pathway is thought to be the main methanogenic pathway in the deep sediment layers (below sulfate penetration) in Eckernförde Bay (Whiticar, 2002). Hydrogenotrophic methanogenesis was determined using ¹⁴C-bicarbonate. At every sampled sediment depth (12 depths in 30 cm intervals), triplicate glass tubes (5 mL) were inserted directly into the sediment. Tubes were filled bubble-free with sediment and closed with butyl rubber stoppers on both ends according to (Treude et al. 2005). Methods following sampling were identical as described in 2.7.2.

2.8 Molecular analysis

In September 2014, additional samples were prepared for the methanol treatment of the 0-1 cmbsf horizon during the potential methanogenesis experiment described in 2.7.3 to detect and quantify the presence of methanogens in the sediment. Therefore, additional 15 vials were prepared with addition of methanol as described in 2.7.3 for five different time points (day 1 (= t₀), day 8, day 16, day 22, and day 36) and stopped at each time point by transferring sediment from the triplicate slurries into whirl-packs (Nasco), which then were immediately frozen at -20°C. DNA was extracted from ~500 mg of sediment using the FastDNA® SPIN Kit for Soil (Biomedical). Quantitative real-time polymerase chain reaction (qPCR) technique using TaqMan probes and TaqMan chemistry (Life



Technologies) was used for the detection of methanogens on a ViiA7 qPCR machine (Life Technologies). Primer and Probe sets as originally published by Yu et al. (2005) were applied to quantify the orders *Methanobacteriales*, *Methanosarcinales* and *Methanomicrobiales* along with the two families *Methanosarcinaceae* and *Methanosaetaceae* within the order *Methanosarcinales*. In addition, a universal primer set for detection of the domain *Archaea* was used (Yu et al. 2005). Absolut quantification of the 16S rDNA from the groups mentioned above was performed with standard dilution series. The standard concentration reached from 10^8 to 10^1 copies per μL . Quantification of the standards and samples was performed in duplicates. Reaction was performed in a final volume of 12.5 μL containing 0.5 μL of each Primer ($10\text{pmol } \mu\text{L}^{-1}$, MWG), 0.25 μL of the respective probe ($10\text{ pmol } \mu\text{L}^{-1}$, Life Technologies), 4 μL H_2O (Roth), 6.25 μL TaqMan Universal Master Mix II (Life Technologies) and 1 μL of sample or standard. Cycling conditions started with initial denaturation and activation step for 10 min at 95°C , followed by 45 cycles of 95°C for 15 sec, 56°C for 30 sec and 60°C for 60 sec. Non-template controls were run in duplicates with water instead of DNA for all primer and probe sets, and remained without any detectable signal after 45 cycles.

2.9 Statistical Analysis

To determine possible environmental controlling parameters on surface methanogenesis, a Principle Component Analysis (PCA) was applied according to the approach described in Gier et al. (2016). Prior to PCA, the dataset was transformed into ranks to assure the same data dimension. In total, two PCAs were conducted. The first PCA was used to test the relation of parameters in the surface sediment (integrated methanogenesis ($0\text{--}5\text{ cm}$, $\text{mmol m}^{-2} \text{d}^{-1}$), POC content (average value from $0\text{--}5\text{ cmbsf}$, wt %), C/N (average value from $0\text{--}5\text{ cmbsf}$, molar) and the bottom water (25 m water depth) (oxygen (μM), temperature ($^\circ\text{C}$), salinity (PSU), chlorophyll ($\mu\text{g L}^{-1}$), methane (nM)). The second PCA was applied on depth profiles of sediment surface methanogenesis ($\text{nmol cm}^{-3} \text{d}^{-1}$), sediment depth (cm), sediment POC content (wt%), sediment C/N ratio (molar), and sampling month (one value per depth profile at a specific month, the later in the year the higher the value). For each PCA, biplots were produced to view data from different angles and to graphically determine a potential positive, negative or zero correlation between methanogenesis rates and the tested variables.

3. Results

3.1 Water column parameters

From March 2013 to September 2014, the water column had a pronounced temporal and spatial variability of temperature, salinity, and oxygen (Fig. 1 and 2). In 2013, temperature of the upper water column increased from March (1°C) to September (16°C), but decreased again in November



(11°C). The temperature of the lower water column increased from March 2013 (2°C) to November 2013 (12°C). In 2014, lowest temperatures of the upper and lower water column were reached in March (4°C). Warmer temperatures of the upper water column were observed in June and September (around 17°C), while the lower water column peaked in September (13°C). Salinity increased over time during 2013, showing the highest salinity of the upper and lower water column in November (18 and 23 PSU, respectively). In 2014, salinity of the upper water column was highest in March and September (both 17 PSU), and lowest in June (13 PSU). The salinity of the lower water column increased from March 2014 (21 PSU) to September 2014 (25 PSU). In both years, June and September showed the most pronounced vertical gradient of temperature and salinity, featuring a pycnocline at around ~14 m water depth. Summer stratification was also seen in the O₂ profiles, which showed O₂ depleted conditions (O₂ < 150 µM) in the lower water column from June to September in both years, reaching concentrations below 1-2 µM (detection limit of CTD sensor) in September of both years (Fig. 1 and 2). The water column was completely ventilated, i.e. homogenized, in March of both years with O₂ concentrations of 300-400 µM down to the sea floor at about 28 m.

380

381 3.2 Sediment geochemistry in MUC cores

Sediment porewater and solid phase geochemistry results for the years 2013 and 2014 are shown in Fig. 1 and 2, respectively.

Sulfate concentrations at the sediment surface ranged between 15-20 mM. Concentration decreased with depth at all sampling months but was never fully depleted until the bottom of the core (18-29 cmbsf, between 2 and 7 mM sulfate). November 2013 showed the strongest decrease from ~20 mM at the top to ~2 mM at the bottom of the core (27 cmbsf).

Opposite to sulfate, methane concentration increased with sediment depth in all sampling months (Fig. 1 and 2). Over the course of a year (i.e. March to November in 2013, and March to September in 2014), maximum methane concentration increased, reaching the highest concentration in November 2013 (~1 mM at 26 cmbsf) and September 2014 (0.2 mM at 23 cmbsf), respectively. Simultaneously, methane profiles became steeper, revealing higher methane concentrations at shallower sediment depth late in the year. Magnitudes of methane concentrations were similar in the respective months of 2013 and 2014.

In all sampling months, sulfide concentration increased with sediment depth (Fig. 1 and 2). Similar to methane, sulfide profiles revealed higher sulfide concentrations at shallower sediment depth together with higher peak concentrations over the course the sampled months in each sampling year. Accordingly, November 2013 (10.5 mM at 15 cmbsf) and in September 2014 (2.8 mM at 15 cmbsf) revealed the highest sulfide concentrations, respectively. September 2014 was the only



sampling month showing a pronounced decrease in sulfide concentration from 15 cmbsf to 21 cmbsf of over 50 %.

DIC concentrations increased with increasing sediment depth at all sampling months. Concomitant with highest sulfide concentrations, highest DIC concentration was detected in November 2013 (26 mM at 27 cmbsf). At the surface, DIC concentrations ranged between 2-3 mM at all sampling months. In June of both years, DIC concentrations were lowest at the deepest sampled depth compared to the other sampling months (16 mM in 2013, 13 mM in 2014).

At all sampling months, POC profiles scattered around 5 ± 0.9 wt % with depth. Only in November 2013, June 2014 and September 2014, POC content exceeded 5 wt % in the upper 0-1 cmbsf (5.9, 5.2 and 5.3 wt %, respectively) with the highest POC content in November 2013. Also in November 2013, surface C/N ratio was lowest of all sampling months (8.6). In general, C/N ratio increased with depth in both years with values around 9 at the surface and values around 10-11 at the deepest sampled sediment depths.

3.3 Sediment geochemistry in gravity cores

Results from sediment porewater and solid phase geochemistry in the gravity core from September 2013 are shown in Fig. 3. Please note that the sediment depth of the gravity core was corrected by comparing the sulfate concentrations at 0 cmbsf in the gravity core with the corresponding sulfate concentration and depth in the MUC core from September 2013 (Fig. 1). The soft surface sediment is often lost during the gravity coring procedure. Through this correction the topmost layer of the gravity core was set at a depth of 14 cmbsf.

Porewater sulfate concentration in the gravity core decreased with depth (i.e. below 0.1 mM at 107 cmbsf) and stayed below 0.1 mM until 324 cmbsf. Sulfate increased slightly (1.9 mM) at the bottom of the core (345 cmbsf). In concert with sulfate, also methane, sulfide, DIC, POC and C/N profiles showed distinct alteration in the profile at 345 cmbsf (see below, Fig. 3). As fluid seepage has not been observed at the Boknis Eck station (Schlüter et al., 2000), these alterations could either indicate a change in sediment properties or result from a sampling artifact from the penetration of seawater through the core catcher into the deepest sediment layer. The latter process is, however, not expected to considerably affect sediment solid phase properties (POC and C/N), and we therefore dismissed this hypothesis.

Methane concentration increased steeply with depth reaching a maximum of 4.8 mM at 76 cmbsf. Concentration stayed around 4.7 mM until 262 cmbsf, followed by a slight decrease until 324 cmbsf (2.8 mM). From 324 cmbsf to 345 cmbsf methane increased again (3.4 mM).

Both sulfide and DIC concentrations increased with depth, showing a maximum at 45 cmbsf (~ 5 mM) and 345 cmbsf (~ 1 mM), respectively. While sulfide decreased after 45 cmbsf to a minimum of ~ 300 μ M at 324 cmbsf, it slightly increased again to ~ 1 mM at 345 cmbsf. In accordance, DIC



concentrations showed a distinct decrease between 324 cmbsf to 345 cmbsf (from 45 mM to 39 mM). While POC concentrations varied around 5 wt % throughout the core, C/N ratio slightly increased with depth, revealing the lowest ratio at the surface (~3) and the highest ratio at the bottom of the core (~13). However, both POC and C/N showed a distinct increase from 324 cmbsf to 345 cmbsf.

3.4 Methanogenesis activity in MUC cores

3.4.1 Net methanogenesis

Net methanogenesis activity was detected throughout the cores at all sampling months (Fig. 1 and 2). Activity measured in MUC cores increased over the course of the year in 2013 and 2014 (that is: March to November in 2013 and March to September in 2014) with lower rates mostly $< 0.1 \text{ nmol cm}^{-3} \text{ d}^{-1}$ in March and higher rates $> 0.2 \text{ nmol cm}^{-3} \text{ d}^{-1}$ in November 2013 and September 2014, respectively. In general, November 2013 revealed highest net methanogenesis rates ($1.3 \text{ nmol cm}^{-3} \text{ d}^{-1}$ at 1-2 cmbsf). Peak rates were detected at the sediment surface (0-1 cmbsf) at all sampling months except for September 2013 where the maximum rates were situated between 10-15 cmbsf. In addition to the surface peaks, net methanogenesis showed subsurface (= below 1 cmbsf until 30 cmbsf) maxima at all sampling months, but with alternating depths (between 10 and 25 cmbsf). Comparison of integrated net methanogenesis rates (0-25 cmbsf) revealed highest rates in September and November 2013 and lowest rates in March 2014 (Fig. 4). A trend of increasing areal net methanogenesis rates from March to September was observed in both years.

3.4.2 Hydrogenotrophic methanogenesis

Hydrogenotrophic methanogenesis activity determined by ^{14}C -bicarbonate incubations of MUC cores is shown in Fig. 1 and 2. In 2013, maximum activity ranged between $0.01\text{-}0.2 \text{ nmol cm}^{-3} \text{ d}^{-1}$, while in 2014 maxima ranged only between 0.01 and $0.05 \text{ nmol cm}^{-3} \text{ d}^{-1}$. In comparison, maximum hydrogenotrophic methanogenesis was up to two orders of magnitude lower compared to net methanogenesis. Only in March 2013 both activities reached a similar range. Overall, hydrogenotrophic methanogenesis increased with depth in March, September, and November 2013 and in March, June, and September 2014. In June 2013, activity decreased with depth, showing the highest rates in the upper 0-5 cmbsf and the lowest at the deepest sampled depth. Concomitant with integrated net methanogenesis, integrated hydrogenotrophic methanogenesis rates (0-25 cmbsf) were high in September 2013, with slightly higher rates in March 2013 (Fig. 4). Lowest areal rates of hydrogenotrophic methanogenesis were seen in June of both years.



Hydrogenotrophic methanogenesis activity in the gravity core is shown in Fig. 3. Highest activity ($\sim 0.7 \text{ nmol cm}^{-3} \text{ d}^{-1}$) was measured at 45 cmbsf and 138 cmbsf, followed by a decrease with increasing sediment depth reaching $0.01 \text{ nmol cm}^{-3} \text{ d}^{-1}$ at the deepest sampled depth (345 cmbsf).

3.4.3 Potential methanogenesis in manipulated experiments

Potential methanogenesis rates in manipulated experiments included either the addition of inhibitors (molybdate for inhibition of sulfate reduction or BES for inhibition of methanogenesis) or the addition of a non-competitive substrate (methanol). Control treatments were run with neither the addition of inhibitors nor the addition of methanol.

Controls. Potential methanogenesis activity in the control treatments was below $0.5 \text{ nmol cm}^{-3} \text{ d}^{-1}$ from March 2014 to September 2014 (Fig. 5). Only in November 2013, control rates exceeded $0.5 \text{ nmol cm}^{-3} \text{ d}^{-1}$ below 6 cmbsf. While rates increased with depth in November 2013 and June 2014, they decreased with depth at the other two sampling months.

Molybdate. Peak potential methanogenesis rates in the molybdate treatments were found in the uppermost sediment interval (0-1 cmbsf) at almost every sampling month with rates being 3-30 times higher compared to the control treatments ($< 0.5 \text{ nmol cm}^{-3} \text{ d}^{-1}$). In November 2013, potential methanogenesis showed two maxima (0-1 and 10-15 cmbsf). Highest measured rates were found in September 2014 ($\sim 6 \text{ nmol cm}^{-3} \text{ d}^{-1}$), followed by November 2013 ($\sim 5 \text{ nmol cm}^{-3} \text{ d}^{-1}$).

BES. Profiles of potential methanogenesis in the BES treatments were similar to the controls mostly in the lower range $< 0.5 \text{ nmol cm}^{-3} \text{ d}^{-1}$. Only in November 2013 rates exceeded $0.5 \text{ nmol cm}^{-3} \text{ d}^{-1}$. Rates increased with depth at all sampling months, except for September 2014, where highest rates were found at the sediment surface (0-1 cmbsf).

Methanol. At all sampling months, potential rates in the methanol treatments were three orders of magnitude higher compared to the control treatments ($< 0.5 \text{ nmol cm}^{-3} \text{ d}^{-1}$). Except for November 2013, potential methanogenesis rates in the methanol treatments were highest in the upper 0-5 cmbsf and decreased with depth. In November 2013, highest rates were detected at the deepest sampled depth (20-25 cmbsf).

3.4.4 Potential methanogenesis determined from ^{13}C -labelled methanol

The concentration of methanol in the sediment decreased sharply in the first 2 weeks from $\sim 8 \text{ mM}$ at day 1 to 0.5 mM at day 13 (Fig. 6). At day 17, methanol was below the detection limit. In the first 2 weeks, residual methanol was enriched with ^{13}C , reaching $\sim 200 \text{ ‰}$ at day 13.

Over the same time period, the concentration of methane increased from 2 ppmv at day 1 to $\sim 66,000 \text{ ppmv}$ at day 17 and stayed around that value until the end of the total incubation time (until day 37) (Fig. 6). The carbon isotopic signature of methane ($\delta^{13}\text{C}_{\text{CH}_4}$) showed a clear enrichment of the heavier isotope ^{13}C (Table 3) from day 9 to 17 (no methane was detectable at day 1). After day 17,



503 $\delta^{13}\text{C}_{\text{CH}_4}$ stayed around 13‰ until the end of the incubation. The concentration of CO_2 in the
 504 headspace increased from ~8900 ppmv at day 1 to ~29,000 ppmv at day 20 and stayed around
 505 30,000 ppmv until the end of the incubation (Fig. 6). Please note, that the major part of CO_2 was
 506 dissolved in the porewater, thus the CO_2 concentration in the headspace does not show the total CO_2
 507 concentration in the system. CO_2 in the headspace was enriched with ^{13}C during the first 2 weeks
 508 (from -16.2 to -7.3 ‰) but then stayed around -11 ‰ until the end of the incubation.

509 3.5 Molecular analysis of benthic methanogens

510 In September 2014, additional samples were run during the methanol treatment (see Sect. 2.7.3) for
 511 the detection of benthic methanogens via qPCR. The qPCR results are shown in Fig. 7. For a better
 512 comparison, the microbial abundances are plotted together with the sediment methane
 513 concentrations from the methanol treatment, from which the rate calculation for the methanol-
 514 methanogenesis at 0-1 cmbsf was done (shown in Fig. 5).

515 Methane concentrations increased over time revealing a slow increase in the first ~10 days, followed
 516 by a steep increase between day 13 and day 20 and ending in a stationary phase.

517 A similar increase was seen in the abundance of total and methanogenic archaea. Total archaea
 518 abundances increased sharply in the second week of the incubation reaching a maximum at day 16
 519 ($\sim 5000 \cdot 10^6$ copies g^{-1}) and stayed around $3000 \cdot 10^6$ - $4000 \cdot 10^6$ copies g^{-1} over the course of the
 520 incubation. Similarly, methanogenic archaea, namely the order *Methanosarcinales* and within this
 521 order the family *Methanosarcinaceae*, showed a sharp increase in the first 2 weeks as well with the
 522 highest abundances at day 16 ($\sim 6 \cdot 10^8$ copies g^{-1} and $\sim 1 \cdot 10^6$ copies g^{-1} , respectively). Until the end of
 523 the incubation, the abundances of *Methanosarcinales* and *Methanosarcinaceae* decreased to about a
 524 third of their maximum abundances ($\sim 2 \cdot 10^8$ copies g^{-1} and $\sim 0.4 \cdot 10^6$ copies g^{-1} , respectively).

525 3.6 Statistical Analysis

526 The PCA of integrated surface methanogenesis (0-5 cmbsf) (Fig.10) showed a strong positive
 527 correlation with bottom water temperature (Fig. 9a), bottom water salinity (Fig. 9a), and surface
 528 sediment POC content (Fig. 9c). Further, a positive correlation with bottom water methane and a
 529 weak positive correlation with surface sediment C/N was detected (Fig. 9b). A strong negative
 530 correlation was found with bottom water oxygen concentration (Fig. 9b). No correlation was found
 531 with bottom water chlorophyll.

532 The PCA of methanogenesis depth profiles showed weak positive correlations with sediment depth
 533 (Fig. 10a) and C/N (Fig. 10b), and showed negative correlations with POC (Fig. 10a).

534



535 4. Discussion

536 4.1 Methanogenesis in the sulfate-reducing zone

537 On the basis of the results presented in Fig. 1 and 2, it is evident that methanogenesis and sulfate
 538 reduction were concurrently active in the surface sediments (0-30 cmbsf) at Boknis Eck. Even though
 539 sulfate reduction rates were not measured directly, the decrease in sulfate concentrations with a
 540 concomitant increase in sulfide within the upper 30 cmbsf indicate that sulfate reduction was active
 541 (Fig. 1 and 2). Several earlier studies in Eckernförde Bay sediments confirmed the dominance of
 542 sulfate reduction in the surface sediment, which revealed an activity of $100\text{--}10000\text{ nmol cm}^{-3}\text{ d}^{-1}$ in
 543 the upper 25 cmbsf (Treude et al., 2005a; Bertics et al., 2013; Dale et al., 2013). Microbial
 544 fermentation of organic matter was probably high in the organic-rich sediments of Eckernförde Bay
 545 (POC contents of around 5 %, Fig. 1 and 2), providing high substrate availability and variety for
 546 methanogenesis.

547
 548 The results of this study further identified methylotrophy to be an important non-competitive
 549 methanogenic pathway in the sulfate-reducing zone. The pathway utilizes alternative substrates,
 550 such as methanol, to avoid competition with sulfate reducers for H_2 and acetate. The relevance of
 551 methylotrophic methanogenesis in the sulfate-reducing zone was supported by the following
 552 observations: 1) Hydrogenotrophic methanogenesis was up to two orders of magnitude lower than
 553 net methanogenesis (Fig. 1 and 2), 2) methanogenesis increased when sulfate reduction was
 554 inhibited (Fig. 5), 3) addition of BES did not result in the inhibition of methanogenesis (Fig. 6), 4)
 555 addition of methanol increased potential methanogenesis rates up to three orders of magnitude (Fig.
 556 6), 5) methylotrophic methanogens of the order *Methanosarcinales* were detected in the methanol-
 557 treatment (Fig. 7), and 6) stable isotope probing revealed highly ^{13}C -enriched methane produced
 558 from ^{13}C -labelled methanol (Fig. 6). In the following chapters, these arguments will be discussed in
 559 more detail.

560 4.1.1 Hydrogenotrophic methanogenesis

561 We demonstrated that hydrogenotrophic methanogenesis was insufficient to explain the observed
 562 net methanogenesis. The only exemption was March 2013, where rates of hydrogenotrophic
 563 methanogenesis exceeded net methanogenesis in discrete depths (5-6 cmbsf and 25-30 cmbsf). It is
 564 possible that additional carbon sources led to increased local fermentation processes, for instance
 565 from the deposition of macro algae detritus, which is produced during winter storms and can be
 566 transported into deeper sediment layers by bioturbation, where it is digested and released as fecal
 567 pellets (Meyer-Reil, 1983; Bertics et al., 2013). Such additional carbon sources from fresh material
 568 could lead to the local accumulation of excess hydrogen through fermentation and reduce the



569 competition for H_2 between sulfate reducers and methanogens (Treude et al., 2009). C/N ratios in
570 March 2013 were more scattered compared to other months in 2013 and 2014, indicating the
571 transport of labile material into the sediment. Eckernförde Bay sediments are known for bioturbation
572 especially during early spring by mollusks and polychaetes (D'Andrea et al., 1996; Orsi et al., 1996;
573 Bertics et al., 2013; Dale et al., 2013), and mollusk shells were observed even at depth of ~ 20 cmbsf
574 during sampling in the present study (personal observation).
575 Hydrogenotrophic methanogenesis was also detected in the gravity core in September 2013.
576 Maximum hydrogenotrophic rates were found at 45 cmbsf and 138 cmbsf, indicating a higher usage
577 of CO_2 and H_2 at depths > 40 cmbsf, where sulfate was depleted and thus the competition between
578 sulfate reducers and methanogens was relieved.

579 4.1.2 Inhibition of sulfate reducers

580 The competition between methanogens and sulfate reducers within the upper 30 cmbsf led to the
581 predominant utilization of non-competitive substrates by methanogenesis, as indicated by low
582 hydrogenotrophic methanogenesis rates (see discussion above). After the addition of the sulfate-
583 reducer inhibitor molybdate, competitive substrates (H_2/CO_2 and acetate (Oremland & Polcin, 1982;
584 King et al., 1983) were available for methanogenesis as indicated by the increase (up to 30 times) in
585 potential activity (Fig. 5 and 6). Notably, highest rates in the molybdate treatment were measured at
586 the shallowest sediment depth at most sampling months (except November 2013), pointing towards
587 the strongest competition between sulfate reducers and methanogens directly at the top 0-1 cmbsf,
588 which is confirmed by sulfate reduction maxima found at 0-1 cmbsf in earlier studies (Bertics et al.
589 2013; Treude et al. 2005).

590 4.1.3 Inhibition of methanogenesis by BES

591 Addition of BES did not result in the expected inhibition of potential methanogenesis; instead rates
592 were in the same range as the control treatment (Fig. 6). Either the inhibition of BES was incomplete,
593 or the methanogens were insensitive to BES (Hoehler et al., 1994; Smith & Mah, 1981; Santoro &
594 Konisky, 1987). However, the BES concentration used in the present study (60 mM) has been shown
595 to result in successful inhibition of methanogens in previous studies (Hoehler et al., 1994). Therefore,
596 the presence of methanogens that are insensitive to BES was more likely. Insensitivity to BES would
597 support the hypothesis that methanogenesis in the sulfate reduction zone is mainly driven via the
598 methylotrophic pathway, as BES resistance was shown in *Methanosarcina* mutants in earlier studies
599 (Smith & Mah, 1981; Santoro & Konisky, 1987), a genus which we successfully detected in our
600 samples (for more details see Sect. 4.1.5), and which is known for mediating the methylotrophic
601 pathway (Keltjens & Vogels, 1993).



4.1.4 Methanol addition

High potential methanogenesis rates observed after the addition of the non-competitive substrate methanol leads to the assumption that non-competitive substrates relieve the competition between methanogens and sulfate reducers in surface sediments of Eckernförde Bay. Except for November 2013, highest rates in the methanol-treatment were detected in the upper 0-5 cmbsf and decreased with depth (Fig. 5). Highest methanogenesis rates in the upper 0-5 cmbsf of the methanol-treatment can be interpreted as follows: (1) The amount of non-competitive substrates including methanol was most likely highest at the sediment surface, as those substrates are derived from fresh organic matter, such as pectin or betaine and dimethylpropiothetin (both osmoprotectants) (Zinder, 1993). (2) Sulfate reduction is most dominant in the 0-5 cmbsf (Treude et al., 2005a; Bertics et al., 2013), which probably leads prevalent methanogens to be more adapted to the usage of non-competitive substrates.

It should be noted that even though methanogenesis rates were calculated assuming a linear increase in methane concentration over the entire incubation to make a better comparison between different treatments, the methanol treatments generally showed a delayed response in methane development (Supplement, Fig. S1). A similar delay was observed in organic-rich surface sediments sampled off Peru and was explained by the predominant use of alternative non-competitive substrates such as methylated sulfides (e.g. dimethyl sulfide or methanethiol (Maltby et al., 2016)). In the marine environment, dimethyl sulfide mainly originates from the algae osmoregulatory compound dimethylsulfoniopropionate (DMSP) (Van Der Maarel & Hansen, 1997), which could have accumulated in Eckernförde Bay sediments, due to intense sedimentation of algae blooms (Bange et al., 2011). Certain *Methanosarcina* species have been shown to use DMS as a substrate (Sieburth et al., 1993; Van Der Maarel & Hansen, 1997), a genus, which has been detected in our samples (see more details under Sect. 4.1.5).

Additionally, there are hints that methylated sulfur compounds may be generated through nucleophilic attack by sulfide on the methyl groups in the sedimentary organic matter (Mitterer, 2010). As shown in the present study, sulfide was an abundant species in the surface sediment (up to mM levels) (Fig. 1 and 2).

4.1.5 Presence of methylotrophic methanogens

Simultaneously with the increase in methane concentration after methanol addition in the surface layer (0-1 cmbsf) in September 2014, the DNA counts for the order *Methanosarcinales* and the family *Methanosarcinaceae* within the order *Methanosarcinales* increased 102 to 10^6 times, respectively, compared to the respective DNA abundances at the start of the incubation (Fig. 7). The successful enrichment of *Methanosarcinaceae* indicates that this family is present in the natural environment and thus could in part be responsible for the observed surface methanogenesis. As the members of



the family *Methanosarcinaceae* are known for utilization of methylated substrates (Boone et al., 1993), our hypothesis for the predominant usage of non-competitive substrates is supported. The delay in growth of *Methanosarcinales* and *Methanosarcinaceae*, however, also hints towards the predominant usage of other non-competitive substrates besides methanol (see also Sect. 4.1.4).

4.1.6 Stable-isotope experiment

Samples taken in September 2014 for the labeling experiment (^{13}C -enriched methanol, initial isotopic signature: +26 ‰) showed that methanol was completely consumed after 17 days and converted to methane and CO_2 , as both revealed a concomitant enrichment in ^{13}C . The production of both methane and CO_2 from methanol has been shown previously in different strains of methylotrophic methanogens (Penger et al., 2012). As mentioned earlier, the major part of CO_2 was dissolved in the porewater, which was not determined isotopically in this study, which is why we neglect the CO_2 development in the following.

Fractionation factors of methylotrophic methanogenesis from methanol to methane have been found to be 1.07–1.08 (Heyer et al., 1976; Krzycki et al., 1987). This fractionation leads to a progressive enrichment of ^{13}C in the residual methanol until all methanol is consumed. Accordingly, methanol was enriched in ^{13}C in the first 13 days, as the consumption of ^{12}C -methanol was preferred by the microbes. The fast conversion of methanol to methane can only be explained by the presence of methylotrophic methanogens (e.g. members of the family *Methanosarcinaceae*, which is known for the methylotrophic pathway (Keltjens & Vogels, 1993). Please note, however, that the storage of the cores (3.5 months) prior to sampling could have led to shifts in the microbial community and thus might not reflect in-situ conditions of the original microbial community in September 2014. The delay in methane production also seen in the stable isotope experiment was, however, only slightly different (methane developed earlier, between day 8 and 12, data not shown) from the non-labeled methanol treatment (between day 10 to 16, Fig. S1), which leads us to the assumption that the storage time at 1°C did not dramatically affect the methanogen community. Similar, in a previous study with arctic sediments, addition of substrates had no stimulatory effect on the rate of methanogenesis or on the methanogen community structure at low temperatures (5°C , (Blake et al., 2015).

4.2 Environmental control of surface methanogenesis

Surface methanogenesis in Eckernförde Bay sediments showed variations throughout the sampling period, which may be influenced by variable environmental factors such as temperature, salinity, oxygen, and organic carbon. In the following, we will discuss the potential impact of those factors on the magnitude and distribution of surface methanogenesis.

4.2.1 Temperature



During the sampling period, bottom water temperatures increased over the course of the year from late winter (March, 3–4 °C) to autumn (November, 12 °C, Fig. 1 and 2). The PCA revealed a strong positive correlation between bottom water temperature and integrated surface methanogenesis (0–5 cmbsf). A temperature experiment conducted with sediment from ~75 cmbsf in September 2014 within a parallel study revealed a mesophilic temperature optimum of methanogenesis (20 °C, data not shown). Whether methanogenesis in surface sediments (0–30 cm) has the same physiology remains speculative. However, AOM organisms, which are closely related to methanogens (Knittel & Boetius, 2009), studied in surface sediments from the same site were confirmed to have a mesophilic physiology, too (Treude et al. 2005).

4.2.2 Salinity and oxygen

From March 2013 to November 2013, and from March 2014 to September 2014, salinity increased in the bottom-near water (25 m) from 19 to 23 PSU and from 22 to 25 PSU (Fig. 1 and 2), respectively, due the pronounced summer stratification in the water column between saline North Sea water and less saline Baltic Sea water (Bange et al., 2011). The PCA detected a strong positive correlation between integrated surface methanogenesis (0–5 cmbsf) and salinity in the bottom-near water (Fig. 9a). This correlation can hardly be explained by salinity alone, as methanogens feature a broad salinity range from freshwater to hypersaline (Zinder, 1993). Even more, methanogenesis often decreases with increasing salinity (Pattnaik et al., 2000), due to the concurrent increase of sulfate, enabling sulfate-reducing bacteria to degrade organic matter prior to hydrogenotrophic and acetoclastic methanogens (Oremland & Polcin, 1982). In fact, we found steep sulfate and sulfide profiles at times of high salinity, indicating the presence of extensive sulfate reduction activity at the sediment-water interface (Fig. 1 and 2). We therefore interpret positive correlation of methanogenesis with salinity as an indirect indicator for a positive correlation with water column stratification and hypoxia development. Accordingly, the PCA revealed a strong negative correlation between oxygen concentration close to the seafloor and surface methanogenesis. In September 2014 bottom water levels probably reached zero levels as sulfide was detected in the bottom-near water (25 m) 6 days after our sampling (H. Bange, pers. comm.). Hypoxia or anoxia in the bottom-near water and the correlated absence of bioturbating and bioirrigating macrofauna (Dale et al., 2013; Bertics et al., 2013) likely increased the habitable zone of methanogens close to the sediment-water interface. Oxygen is an important factor controlling methanogenesis, as benthic methane is mostly produced under strictly anoxic, highly reducing (< -200 mV) conditions (Oremland, 1988; Zinder, 1993).

4.2.4 Particulate organic carbon



706 The supply of particulate organic carbon (POC) is one of the most important factors controlling
707 benthic heterotrophic processes, as it determines substrate availability and variety (Jørgensen,
708 2006). In Eckernförde Bay, the organic material reaching the sediment floor originates mainly from
709 phytoplankton blooms in spring, summer and autumn (Bange et al., 2011). It has been estimated that
710 > 50 % in spring (February/March), > 25 % in summer (July/August) and > 75 % in autumn
711 (September/October) of these blooms is reaching the seafloor (Smetacek et al., 1984), resulting in a
712 overall high organic carbon content of the sediment (5 wt %), which leads to high benthic microbial
713 degradation rates including sulfate reduction and methanogenesis (Whiticar, 2002; Treude et al.,
714 2005a; Bertics et al., 2013). Previous studies revealed that high organic matter availability can relieve
715 competition between sulfate reducers and methanogens in sulfate-containing, marine sediments
716 (Oremland et al., 1982; Holmer & Kristensen, 1994; Treude et al., 2009; Maltby et al., 2016).
717 To determine the effect of POC concentration and C/N ratio (as a negative indicator for the freshness
718 of POC) on surface methanogenesis, two PCAs were conducted with a) the focus on the upper 0-5
719 cmbsf, which is directly influenced by freshly sedimented organic material from the water column
720 (Fig. 9), and b) the focus on the depth profiles throughout the sediment cores (up to 30 cmbsf) (Fig.
721 10).
722 For the upper 0-5 cmbsf in the sediment, a strong positive correlation was found between surface
723 methanogenesis (integrated) and POC content (averaged) (Fig. 9c), indicating that POC content is an
724 important controlling factor for methanogenesis in this layer. In support, highest bottom-near water
725 chlorophyll concentrations coincided with highest bottom-near water methane concentrations and
726 high integrated surface methanogenesis (0-5 cmbsf) in September 2013, probably as a result of the
727 sedimentation of the summer phytoplankton bloom (Fig. 8). Indeed, the PCA revealed a strong
728 positive correlation between integrated surface methanogenesis rates and bottom-near water
729 methane concentrations (Fig. 9b) viewed over all investigated months. However, no correlation was
730 found between bottom water chlorophyll and integrated surface methanogenesis rates (Fig. 9). As
731 seen in Fig. 8, bottom-near high chlorophyll concentrations did not coincide with high bottom-near
732 methane concentration in June/September 2014. We explain this result by a time lag between
733 primary production in the water column and the export of the produced organic material to the
734 seafloor, which was probably even more delayed during stratification. Such a delay was observed in a
735 previous study (Bange et al., 2010), revealing enhanced water methane concentration close to the
736 seafloor approximately one month after the chlorophyll maximum. The C/N ratio (averaged over 0-5
737 cmbsf) showed a weak positive correlation with integrated surface methanogenesis (0-5 cmbsf),
738 which is surprising as we expected that a higher C/N ratio, indicative for less labile organic carbon,
739 should have a negative effect on non-competitive methanogenesis. However, methanogens are not
740 able to directly use most of the labile organic matter due their inability to process large molecules



741 (more than two C-C bondings) (Zinder, 1993). Methanogens are dependent on other microbial
742 groups to degrade large organic compounds (e.g. amino acids) for them (Zinder, 1993). Because of
743 this substrate speciation and dependence, a delay between the sedimentation of fresh, labile organic
744 matter and the increase in methanogenesis can be expected, which would not be captured by the
745 applied PCA.

746 In the PCA for the surface sediment profiles (0-30 cmbsf), POC showed a negative correlation with
747 methanogenesis, and sediment depth and C/N ratio showed a weak positive correlation with
748 methanogenesis (Fig 10.), which was also seen previously in the weak positive correlation between
749 integrated surface methanogenesis (0-5 cmbsf) and surface C/N (0-5 cmbsf). As POC, with the
750 exemption of the topmost sediment layer, remained basically unchanged over the top 30 cmbsf, its
751 negative correlation with methanogenesis is probably solely explained by the increase of
752 methanogenesis with sediment depth, and can therefore be excluded as a major controlling factor.
753 As sulfate in this zone was likely never depleted to levels that are critically limiting sulfate reduction
754 (lowest concentration 1300 μ M, compare e.g. with Treude et al., 2014) we do not expect a significant
755 change in the competition between methanogens and sulfate reducers. It is therefore more likely
756 that the progressive degradation of organic matter into methanogenic substrates over depth and
757 time had a positive impact on methanogenesis. The C/N ratio indicates such a trend as the labile
758 fraction of POC decreased with depth. The mobilization of dissolved methanogenic substrates, such
759 as methanol, from organic matter would not be detectable by the C/N ratio as it is determined from
760 particulate samples.

761 4.3 Relevance of surface methanogenesis in Eckernförde Bay sediments

762 The time series station Boknis Eck in Eckernförde Bay is known for being a methane source to the
763 atmosphere throughout the year due to supersaturated waters, which result from significant benthic
764 methanogenesis and emission (Bange et al., 2010). The benthic methane formation is thought to take
765 place mainly in the deeper, sulfate-depleted sediment layers (Treude et al., 2005a; Whiticar, 2002).

766 In the present study, we show that surface methanogenesis within the sulfate zone is present despite
767 sulfate concentrations > 1 mM, a limit above which methanogenesis has been thought to be
768 negligible (Alperin et al., 1994; Hoehler et al., 1994; Burdige, 2006), and thus could contribute to
769 benthic methane emissions. In support of this hypothesis, high dissolved methane concentration in
770 the water column occurred with concomitant high surface methanogenesis activity (Fig. 8).

771 In fact, surface methanogenesis in the Eckernförde Bay could even increase in the future, as
772 temperature and oxygen, two important controlling factors identified for surface methanogenesis
773 (Maltby et al., 2016) and this study), are predicted to increase and decrease, respectively (Lennartz et
774 al., 2014). We will therefore have a closer look at the magnitude and potential relevance of this
775 process for methane the benthic methane budget.



776 Surface methanogenesis rates determined in the present study are in a similar range of other sulfate-
 777 containing, organic-rich surface sediments (e.g. salt marsh sediments, sediments from the upwelling
 778 region off Chile and Peru, or coastal sediments from Limfjorden, North Sea), (Table 2, References
 779 herein). In comparison with methanogenesis rates below the sulfate-methane- transition zone
 780 (SMTZ) of organic-rich sediments (coastal and upwelling sediments), rates were mainly lower (2-5
 781 times) (Table 2), which is explained by the competition relief below the SMTZ, which makes more
 782 substrates available for methanogenesis.

783 We also performed a comparison between surface (0-30 cmbsf) and deep (below the SMTZ) net
 784 methanogenesis for the present study site to investigate the relevance of surface methanogenesis in
 785 Eckernförde Bay sediments for the overall benthic methane budget. In the gravity core of September
 786 2013, the SMTZ was situated between 45 and 76 cmbsf (Fig. 3). The methane flux was estimated
 787 according to Iversen & Jørgensen, (1993) using a sediment methane diffusion coefficient of $D_s =$
 788 $1.64 \times 10^{-5} \text{ cm}^2 \text{ s}^{-1}$. The sediment diffusion coefficient was derived from the seawater methane-
 789 diffusion coefficient at 10 °C (Schulz, 2006), which was corrected by porosity according to Iversen &
 790 Jørgensen, (1993). The calculated deep methane production ($1.55 \text{ mmol m}^{-2} \text{ d}^{-1}$) was similar to earlier
 791 calculated deep methanogenesis in Eckernförde Bay ($0.66 - 1.88 \text{ mmol m}^{-2} \text{ d}^{-1}$; Treude et al., 2005a).
 792 However, integrated hydrogenotrophic methanogenesis measured in the presented study below 45
 793 cmbsf (determined by interpolation, $0.5 \pm 0.2 \text{ mmol m}^{-2} \text{ d}^{-1}$) was up to 3 times lower compared to the
 794 calculated deep methanogenesis, indicating that the interpolation missed hot spots of
 795 hydrogenotrophic methanogenesis, as alternative pathways are not predicted for this zone given the
 796 isotopic signature of methane (Whiticar, 2002). Surface methanogenesis in September 2013
 797 represented 3-8 % of deep methanogenesis. While this percentage seems low, absolute surface
 798 methanogenesis rates in Eckernförde Bay sediments are in the same magnitude as deep methane
 799 production in other organic-rich sediments from the North Sea ($0.076 \text{ mmol m}^{-2} \text{ d}^{-1}$, Jørgensen &
 800 Parkes, 2010), or from the upwelling region off Chile ($0.068\text{-}0.13 \text{ mmol m}^{-2} \text{ d}^{-1}$, Treude et al., 2005b),
 801 indicating the general importance of this process. Compared to these other sites, Eckernförde Bay
 802 features extremely high methanogenesis activity below the SMTZ, resulting in gas bubble formation
 803 and ebullition (Abegg & Anderson, 1997; Jackson et al., 1998; Treude et al., 2005a).
 804 How much of methane produced in the surface sediment is emitted into the water column depends
 805 on the rate of methane consumption, i.e., aerobic and anaerobic oxidation of methane in the
 806 sediment (Knittel & Boetius, 2009). In organic-rich sediments such as in the presented study, the oxic
 807 sediment layer is often only mm-thick, due to the high rates of microbial organic matter degradation,
 808 which rapidly consumes oxygen (Revsbech et al., 1980; Emerson et al., 1985; Jørgensen, 2006). Thus
 809 the anaerobic oxidation of methane (AOM) might play a more dominant role in the present study. In
 810 an earlier study from Eckernförde Bay, AOM rates were measured above the SMTZ (0-25 cmbsf), but



811 the authors concluded that it was fueled by deep methanogenesis (Treude et al., 2005a), as surface
812 integrated AOM rates ($0.8\text{--}1.5\text{ mmol m}^{-2}\text{ d}^{-1}$) were in the same magnitude as deep methane flux
813 ($0.66\text{--}1.88\text{ mmol m}^{-2}\text{ d}^{-1}$) from below the SMTZ (Treude et al., 2005a).
814 With the data set presented here we postulate that surface AOM above the SMTZ ($0.8\text{ mmol m}^{-2}\text{ d}^{-1}$,
815 Treude et al., (2005a) is mainly fueled by surface methanogenesis. If this is the case, then surface
816 methanogenesis is more likely in the range of $0.9\text{ mmol m}^{-2}\text{ d}^{-1}$ (AOM + net surface methanogenesis),
817 indicating that surface methanogenesis could play a much bigger role for benthic methane budgeting
818 than previously thought. Whether surface methanogenesis at Eckernförde Bay has the potential for
819 direct methane emissions into the water column goes beyond the informative nature of our dataset
820 and should be tested in future studies. Our study shows that surface methanogenesis correlates with
821 methane concentrations in the water column near the seafloor; however, so could also
822 methanogenesis and gas ebullition from below the SMTZ.

823 5. Summary

824 The present study demonstrated that methanogenesis and sulfate reduction were concurrently
825 active within the sulfate-reducing zone in sediments at Boknis Eck (Eckernförde Bay, SW Baltic Sea).
826 Observed methanogenesis was probably based on non-competitive substrates due to the
827 competition with sulfate reducers for the substrates H_2 and acetate. Accordingly, members of the
828 family *Methanosarcinaceae*, which are known for methylotrophic methanogenesis and were found in
829 the surface sediments, are likely to be responsible for the observed surface methanogenesis using
830 the substrates methanol, methylamines or methylated sulfides.
831 An important factor controlling surface methanogenesis in the upper 0-5 cmbsf was the POC content,
832 resulting in highest methanogenesis activity after summer and autumn phytoplankton blooms.
833 Increased stratification (indicated by increased salinity at the seafloor) was also found to be
834 beneficial for surface methanogenesis, as it leads the decline of oxygen below the pycnocline.
835 Accordingly, oxygen depletion during later summer showed a strong positive correlation with surface
836 methanogenesis, enabling more organic matter to reach the seafloor and providing a larger habitable
837 anoxic zone for methanogens in the surface sediment.
838 With increasing sediment depth (0-30 cmbsf), methanogenesis revealed only a positive correlation
839 with C/N ratio, indicating that a progressive mobilization of dissolved methanogenic substrates from
840 fermentation plays an important role for controlling non-competitive methanogenesis.
841 Even though surface methanogenesis was low compared to methanogenesis below the STTZ, it may
842 play an underestimated role in the methane budget at Boknis Eck, e.g., by directly fueling AOM
843 above the SMTZ.



844 **Author Contribution**

845 J.M. and T.T. designed the experiments. J.M. carried out all experiments. H.W. coordinated
846 measurements of water column methane and chlorophyll. C.L. and M.F. conducted molecular
847 analysis. M.S. coordinated ¹³C-Isotope measurements. J.M. prepared the manuscript with
848 contributions from all co-authors.

849 **Data Availability**

850 Research data for the present study can be accessed via the public data repository PANGAEA
851 (doi:10.1594/PANGAEA.873185).

852 **Acknowledgements**

853 We thank the captain and crew of F.S. Alkor, F.K. Littorina and F.B. Polarfuchs for field assistance. We
854 thank G. Schüssler, F. Wulff, P. Wefers, A. Petersen, M. Lange, and F. Evers for field and laboratory
855 assistance. For the geochemical analysis we want to thank B. Domeyer, A. Bleyer, U. Lomnitz, R.
856 Suhrberg, and V. Thoenissen. We thank F. Malien, X. Ma, A. Kock and T. Baustian for the O₂, CH₄, and
857 chlorophyll measurements from the regular monthly Boknis Eck sampling cruises. Further we thank
858 R. Conrad and P. Claus at the MPI Marburg for the ¹³C-Methanol measurements. This study received
859 financial support through the Cluster of Excellence “The Future Ocean” funded by the German
860 Research Foundation, through the Sonderforschungsbereich (SFB) 754, and through a D-A-CH project
861 funded by the Swiss National Science Foundation and German Research foundation (grant no.
862 200021L_138057, 200020_159878/1). Further support was provided through the EU COST Action
863 PERGAMON (ESSEM 0902), through the BMBF project BioPara (grant no. 03SF0421B) and through
864 the EU’s H2020 program (Marie Curie grant NITROX # 704272 to CRL).

865

866 **References**

- 867 Abegg, F. & Anderson, A.L. (1997). The acoustic turbid layer in muddy sediments of Eckernförde Bay
868 , Western Baltic : methane concentration , saturation and bubble characteristics. *Marine*
869 *Geology*. 137. pp. 137–147.
- 870 Alperin, M.J., Albert, D.B. & Martens, C.S. (1994). Seasonal variations in production and consumption
871 rates of dissolved organic carbon in an organic-rich coastal sediment. *Geochimica et*
872 *Cosmochimica Acta*. 58 (22). pp. 4909–4930.
- 873 Bakker, D.E., Bange, H.W., Gruber, N., Johannessen, T., Upstill-Goddard, R.C., Borges, A.V., Delille, B.,
874 Löscher, C.R., Naqvi, S.W.A., Omar, A.M. & Santana-Casiano-J.M. (2014). Air-sea interactions of
875 natural long-lived greenhouse gases (CO₂, N₂O, CH₄) in a changing climate. In: P. S. Liss & M. T.
876 Johnson (eds.). *Ocean-Atmosphere Interactions of Gases and Particles*. Heidelberg: Springer-
877 Verlag, pp. 113–169.
- 878 Balzer, W., Pollehne, F. & Erlenkeuser, H. (1986). Cycling of Organic Carbon in a Marine Coastal
879 System. In: P. G. Sly (ed.). *Sediments and Water Interactions*. New York, NY: Springer New York,



- 880 pp. 325–330.
- 881 Bange, H.W., Bartell, U.H., Rapsomanikis, S. & Andreae, M.O. (1994). Methane in the Baltic and North
882 Seas and a reassessment of the marine emissions of methane. *Global Biogeochemical Cycles*. 8
883 (4). pp. 465–480.
- 884 Bange, H.W., Bergmann, K., Hansen, H.P., Kock, A., Koppe, R., Malien, F. & Ostrau, C. (2010).
885 Dissolved methane during hypoxic events at the Boknis Eck time series station (Eckernförde
886 Bay , SW Baltic Sea). *Biogeosciences*. 7. pp. 1279–1284.
- 887 Bange, H.W., Hansen, H.P., Malien, F., Laß, K., Karstensen, J., Petereit, C., Friedrichs, G. & Dale, A.
888 (2011). Boknis Eck Time Series Station (SW Baltic Sea): Measurements from 1957 to 2010.
889 *LOICZ-Affiliated Activities*. Inprint 20. pp. 16–22.
- 890 Bertics, V.J., Löscher, C.R., Salonen, I., Dale, A.W., Gier, J., Schmitz, R.A. & Treude, T. (2013).
891 Occurrence of benthic microbial nitrogen fixation coupled to sulfate reduction in the seasonally
892 hypoxic Eckernförde Bay, Baltic Sea. *Biogeosciences*. 10 (3). pp. 1243–1258.
- 893 Blake, L.I., Tveit, A., Øvreås, L., Head, I.M. & Gray, N.D. (2015). *Response of Methanogens in Arctic*
894 *Sediments to Temperature and Methanogenic Substrate Availability*.
- 895 Buckley, D.H., Baumgartner, L.K. & Visscher, P.T. (2008). Vertical distribution of methane metabolism
896 in microbial mats of the Great Sippewissett Salt Marsh. *Environmental microbiology*. 10 (4). pp.
897 967–77.
- 898 Burdige, D.J. (2006). *Geochemistry of Marine Sediments*. New Jersey, U.S.A.: Princeton University
899 Press.
- 900 Cicerone, R.J. & Oremland, R.S. (1988). Biogeochemical aspects of atmospheric methane. *Global*
901 *Biogeochemical Cycles*. 2 (4). pp. 299–327.
- 902 Crill, P.M. & Martens, C.S. (1986). Methane production from bicarbonate and acetate in an anoxic
903 marine sediment. *Geochimica et Cosmochimica Acta*. 50. pp. 2089–2097.
- 904 D’Andrea, a. F., Craig, N.I. & Lopez, G.R. (1996). Benthic macrofauna and depth of bioturbation in
905 Eckernförde Bay, southwestern Baltic Sea. *Geo-Marine Letters*. 16 (3). pp. 155–159.
- 906 Dale, a. W., Bertics, V.J., Treude, T., Sommer, S. & Wallmann, K. (2013). Modeling benthic–pelagic
907 nutrient exchange processes and porewater distributions in a seasonally hypoxic sediment:
908 evidence for massive phosphate release by Beggiatoa? *Biogeosciences*. 10 (2). pp. 629–651.
- 909 Denman, K.L., Brasseur, G., Chidthaisong, A., Ciais, P., Cox, P.M., Dickinson, R.E., Hauglustaine, D.,
910 Heinze, C., Holland, E., Jacob, D., Lohmann, U., Ramachandran, S., da Silva Dias, P.L., Wofsy, S.C.
911 & Zhang, X. (2007). Couplings Between Changes in the Climate System and Biogeochemistry. In:
912 S. Solomon, D. Qin, M. Manning, Z. Chen, M. Marquis, K. B. Averyt, M. Tignor, & H. L. Miller
913 (eds.). *Climate Change 2007: The Physical Science Basis. Contribution of Working Group I to the*
914 *Fourth Assessment Report of the Intergovernmental Panel on Climate Change*. Cambridge,
915 United Kingdom and New York, NY, USA: Cambridge University Press.
- 916 Emerson, S., Fischer, K., Reimers, C. & Heggie, D. (1985). Organic carbon dynamics and preservation
917 in deep-sea sediments. *Deep Sea Research Part A. Oceanographic Research Papers*. 32 (1). pp.
918 1–21.
- 919 EPA (2010). *Methane and nitrous oxide emissions from natural sources*. Washington, DC, USA.
- 920 Ferdelman, T.G., Lee, C., Pantoja, S., Harder, J., Bebout, B.M. & Fossing, H. (1997). Sulfate reduction
921 and methanogenesis in a Thioploca-dominated sediment off the coast of Chile. *Geochimica et*
922 *Cosmochimica Acta*. 61 (15). pp. 3065–3079.
- 923 Gier, J., Sommer, S., Löscher, C.R., Dale, A.W., Schmitz, R.A. & Treude, T. (2016). Nitrogen fixation in
924 sediments along a depth transect through the Peruvian oxygen minimum zone. *Biogeosciences*.
925 13 (14). pp. 4065–4080.



- 926 Grasshoff, K., Ehrhardt, M. & Kremmling, K. (1999). *Methods of Seawater Analysis*. Weinheim: Verlag
927 Chemie.
- 928 Hansen, H.-P., Giesenhausen, H.C. & Behrends, G. (1999). Seasonal and long-term control of bottom-
929 water oxygen deficiency in a stratified shallow-water coastal system. *ICES Journal of Marine*
930 *Science*. 56. pp. 65–71.
- 931 Hartmann, D.L., Klein Tank, A.M.G., Rusticucci, M., Alexander, L.V., Brönnimann, S., Charabi, Y.,
932 Dentener, F.J., Dlugokencky, D.R., Easterling, D.R., Kaplan, A., Soden, B.J., Thorne, P.W., Wild,
933 M. & Zhai, P.M. (2013). Observations: Atmosphere and Surface. In: *Climate Change 2013: The*
934 *pHysical Science Basis. Contribution Group I to the Fifth Assessment Report of the*
935 *Intergovernmental Panel on Climate Change*. United Kingdom and New York, NY, USA:
936 Cambridge University Press.
- 937 Heyer, J., Hübner, H. & Maaß, I. (1976). Isotopenfraktionierung des Kohlenstoffs bei der mikrobiellen
938 Methanbildung. *Isotopenpraxis Isotopes in Environmental and Health Studies*. [Online]. 12 (5).
939 pp. 202–205. Available from:
940 <http://www.tandfonline.com/doi/abs/10.1080/10256017608543912>. [Accessed: 15 October
941 2014].
- 942 Hoehler, T.M., Alperin, M.J., Albert, D.B. & Martens, C.S. (1994). Field and laboratory studies of
943 methane oxidation in an anoxic marine sediment: Evidence for a methanogen-sulfate reducer
944 consortium. *Global Biogeochemical Cycles*. 8 (4). pp. 451–463.
- 945 Holmer, M. & Kristensen, E. (1994). Coexistence of sulfate reduction and methane production in an
946 organic-rich sediment. *Marine Ecology Progress Series*. 107. pp. 177–184.
- 947 Iversen, N. & Jørgensen, B.B. (1993). Diffusion coefficients of sulfate and methane in marine
948 sediments: Influence of porosity. *Geochimica et Cosmochimica Acta*. 57 (3). pp. 571–578.
- 949 Jackson, D.R., Williams, K.L., Wever, T.F., Friedrichs, C.T. & Wright, L.D. (1998). Sonar evidence for
950 methane ebullition in Eckernförde Bay. *Continental Shelf Research*. 18. pp. 1893–1915.
- 951 Jørgensen, B.B. (2006). Bacteria and marine Biogeochemistry. In: H. D. Schulz & M. Zabel (eds.).
952 *Marine Geochemistry*. Berlin/Heidelberg: Springer-Verlag, pp. 173–207.
- 953 Jørgensen, B.B. & Parkes, R.J. (2010). Role of sulfate reduction and methane production by organic
954 carbon degradation in eutrophic fjord sediments (Limfjorden, Denmark). *Limnology and*
955 *Oceanography*. 55 (3). pp. 1338–1352.
- 956 Keltjens, J.T. & Vogels, G.D. (1993). Conversion of methanol and methylamines to methane and
957 carbon dioxide. In: J. G. Ferry (ed.). *Methanogenesis: Ecology, Physiology, Biochemistry &*
958 *Genetics*. Chapman & Hall, pp. 253–303.
- 959 King, G.M., Klug, M.J. & Lovley, D.R. (1983). Metabolism of acetate, methanol, and methylated
960 amines in intertidal sediments of lowes cove, maine. *Applied and environmental microbiology*.
961 45 (6). pp. 1848–1853.
- 962 Knittel, K. & Boetius, A. (2009). Anaerobic oxidation of methane: progress with an unknown process.
963 *Annual review of microbiology*. 63. pp. 311–34.
- 964 Krzycki, J.A., Kenealy, W.R., Deniro, M.J. & Zeikus, J.G. (1987). Stable Carbon Isotope Fractionation by
965 *Methanosarcina barkeri* during Methanogenesis from Acetate , Methanol , or Carbon Dioxide-
966 Hydrogen. *Applied and environmental microbiology*. 53 (10).
- 967 Kuivila, K.M., Murray, J.W. & Devol, a. H. (1990). Methane production in the sulfate-depleted
968 sediments of two marine basins. *Geochimica et Cosmochimica Acta*. 54. pp. 403–411.
- 969 Lennartz, S.T., Lehmann, A., Herrford, J., Malien, F., Hansen, H.-P., Biester, H. & Bange, H.W. (2014).
970 Long-term trends at the Boknis Eck time series station (Baltic Sea), 1957–2013: does climate
971 change counteract the decline in eutrophication? *Biogeosciences*. 11 (22). pp. 6323–6339.



- 972 Van Der Maarel, M.J.E.C. & Hansen, T. a. (1997). Dimethylsulfoniopropionate in anoxic intertidal
973 sediments: A precursor of methanogenesis via dimethyl sulfide, methanethiol, and
974 methiolpropionate. *Marine Geology*. 137 (1–2). pp. 5–12.
- 975 Maltby, J., Sommer, S., Dale, A.W. & Treude, T. (2016). Microbial methanogenesis in the sulfate-
976 reducing zone of surface sediments traversing the Peruvian margin. *Biogeosciences*. 13. pp.
977 283–299.
- 978 Martens, C.S., Albert, D.B. & Alperin, M.J. (1998). Biogeochemical processes controlling methane in
979 gassy coastal sediments---Part 1. A model coupling organic matter flux to gas production ,
980 oxidation and transport. *Continental Shelf Research*. 18. pp. 14–15.
- 981 Meyer-Reil, L.-A. (1983). Benthic response to sedimentation events during autumn to spring at a
982 shallow water station in the Western Kiel Bight. *Marine Biology*. 77. pp. 247–256.
- 983 Mitterer, R.M. (2010). Methanogenesis and sulfate reduction in marine sediments: A new model.
984 *Earth and Planetary Science Letters*. 295 (3–4). pp. 358–366.
- 985 Naqvi, S.W. a., Bange, H.W., Fariás, L., Monteiro, P.M.S., Scranton, M.I. & Zhang, J. (2010). Marine
986 hypoxia/anoxia as a source of CH₄ and N₂O. *Biogeosciences*. 7 (7). pp. 2159–2190.
- 987 Oremland, R.S. (1988). Biogeochemistry of methanogenic bacteria. In: A. J. B. Zehnder (ed.). *Biology*
988 *of Anaerobic Microorganisms*. New York: J. Wiley & Sons, pp. 641–705.
- 989 Oremland, R.S. & Capone, D.G. (1988). Use of specific inhibitors in biogeochemistry and microbial
990 ecology. In: K. C. Marshall (ed.). *Advances in Microbial Ecology*. Advances in Microbial Ecology.
991 Boston, MA: Springer US, pp. 285–383.
- 992 Oremland, R.S., Marsh, L.M. & Polcin, S. (1982). Methane production and simultaneous sulfate
993 reduction in anoxic, salt-marsh sediments. *Nature*. 286. pp. 143–145.
- 994 Oremland, R.S. & Polcin, S. (1982). Methanogenesis and Sulfate Reduction : Competitive and
995 Noncompetitive Substrates in Estuarine Sediments. *Applied and Environmental Microbiology*. 44
996 (6). pp. 1270–1276.
- 997 Orsi, T.H., Werner, F., Milkert, D., Anderson, a. L. & Bryant, W.R. (1996). Environmental overview of
998 Eckernförde Bay, northern Germany. *Geo-Marine Letters*. 16 (3). pp. 140–147.
- 999 Pattnaik, P., Mishra, S.R., Bharati, K., Mohanty, S.R., Sethunathan, N. & Adhya, T.K. (2000). Influence
1000 of salinity on methanogenesis and associated microflora in tropical rice soils. *Microbiological*
1001 *research*. [Online]. 155 (3). pp. 215–220. Available from: [http://dx.doi.org/10.1016/S0944-](http://dx.doi.org/10.1016/S0944-5013(00)80035-X)
1002 [5013\(00\)80035-X](http://dx.doi.org/10.1016/S0944-5013(00)80035-X).
- 1003 Penger, J., Conrad, R. & Blaser, M. (2012). Stable carbon isotope fractionation by methylotrophic
1004 methanogenic archaea. *Applied and environmental microbiology*. [Online]. 78 (21). pp. 7596–
1005 602. Available from:
1006 <http://www.pubmedcentral.nih.gov/articlerender.fcgi?artid=3485729&tool=pmcentrez&render>
1007 [type=abstract](http://www.pubmedcentral.nih.gov/articlerender.fcgi?artid=3485729&tool=pmcentrez&render). [Accessed: 13 October 2014].
- 1008 Pimenov, N., Davidova, I., Belyaev, S., Lein, A. & Ivanov, M. (1993). Microbiological processes in
1009 marine sediments in the Zaire River Delta and the Benguela upwelling region. *Geomicrobiology*
1010 *Journal*. 11 (3–4). pp. 157–174.
- 1011 Preisler, A., de Beer, D., Lichtschlag, A., Lavik, G., Boetius, A. & Jørgensen, B.B. (2007). Biological and
1012 chemical sulfide oxidation in a Beggiatoa inhabited marine sediment. *The ISME journal*. 1 (4).
1013 pp. 341–353.
- 1014 Reeburgh, W. (2007). Oceanic methane biogeochemistry. *Chemical Reviews*. pp. 486–513.
- 1015 Revsbech, N.P., Jørgensen, B.B. & Blackburn, T.H. (1980). Oxygen in the sea bottom measured with a
1016 microelectrode. *Science*. 207 (4437). pp. 1355–1356.
- 1017 Santoro, N. & Konisky, J. (1987). Characterization of bromoethanesulfonate-resistant mutants of



- 1018 Methanococcus voltae: Evidence of a coenzyme M transport system. *Journal of Bacteriology*.
- 1019 169 (2). pp. 660–665.
- 1020 Schlüter, M., Sauter, E., Hansen, H.-P. & Suess, E. (2000). Seasonal variations of bioirrigation in
- 1021 coastal sediments: modelling of field data. *Geochimica et Cosmochimica Acta*. 64 (5). pp. 821–
- 1022 834.
- 1023 Schulz, H.D. (2006). Quantification of early diagenesis: dissolved constituents in marine pore water.
- 1024 In: H. D. Schulz & M. Zabel (eds.). *Marine Geochemistry*. Berlin, Heidelberg: Springer Berlin
- 1025 Heidelberg, pp. 75–124.
- 1026 Seeberg-Elverfeldt, J., Schluter, M., Feseker, T. & Kolling, M. (2005). Rhizon sampling of porewaters
- 1027 near the sediment-water interface of aquatic systems. *Limnology and Oceanography-Methods*.
- 1028 3. pp. 361–371.
- 1029 Senior, E., Lindström, E.B., Banat, I.M. & Nedwell, D.B. (1982). Sulfate reduction and methanogenesis
- 1030 in the sediment of a saltmarsh on the East coast of the United kingdom. *Applied and*
- 1031 *environmental microbiology*. 43 (5). pp. 987–996.
- 1032 Sieburth, J.M., Johnson, P.W., Macario, a. J.L. & De Macario, E.C. (1993). C1 bacteria in the water
- 1033 column of Chesapeake Bay, USA. II. The dominant O₂- and H₂S-tolerant methylotrophic
- 1034 methanogens, coenriched with their oxidative and sulphate reducing bacterial consort, are all
- 1035 new immunotypes and probably include new taxa. *Marine Ecology Progress Series*. 95 (1–2). pp.
- 1036 81–89.
- 1037 Smetacek, V. (1985). The Annual Cycle of Kiel Bight Plankton: A Long-Term Analysis. *Estuaries*. 8
- 1038 (June). pp. 145–157.
- 1039 Smetacek, V., von Bodungen, B., Knoppers, B., Peinert, R., Pollehne, F., Stegmann, P. & Zeitzschel, B.
- 1040 (1984). Seasonal stages characterizing the annual cycle of an inshore pelagic system. *Rapports*
- 1041 *et Proces-Verbaux des Reunions Conseil International pour l'Exploration de la Mer*. 186. pp.
- 1042 126–135.
- 1043 Smith, M.R. & Mah, R. a. (1981). 2-Bromoethanesulfonate: A selective agent for isolating
- 1044 resistant Methanosarcina mutants. *Current Microbiology*. 6 (5). pp. 321–326.
- 1045 Thießen, O., Schmidt, M., Theilen, F., Schmitt, M. & Klein, G. (2006). Methane formation and
- 1046 distribution of acoustic turbidity in organic-rich surface sediments in the Arkona Basin, Baltic
- 1047 Sea. *Continental Shelf Research*. 26 (19). pp. 2469–2483.
- 1048 Treude, T., Krause, S., Maltby, J., Dale, A.W., Coffin, R. & Hamdan, L.J. (2014). Sulfate reduction and
- 1049 methane oxidation activity below the sulfate-methane transition zone in Alaskan Beaufort Sea
- 1050 continental margin sediments: Implications for deep sulfur cycling. *Geochimica et*
- 1051 *Cosmochimica Acta*. 144. pp. 217–237.
- 1052 Treude, T., Krüger, M., Boetius, A. & Jørgensen, B.B. (2005a). Environmental control on anaerobic
- 1053 oxidation of methane in the gassy sediments of Eckernförde Bay (German Baltic). *Limnology*
- 1054 *and Oceanography*. 50 (6). pp. 1771–1786.
- 1055 Treude, T., Niggemann, J., Kallmeyer, J., Wintersteller, P., Schubert, C.J., Boetius, A. & Jørgensen, B.B.
- 1056 (2005b). Anaerobic oxidation of methane and sulfate reduction along the Chilean continental
- 1057 margin. *Geochimica et Cosmochimica Acta*. 69 (11). pp. 2767–2779.
- 1058 Treude, T., Smith, C.R., Wenzhöfer, F., Carney, E., Bernardino, A.F., Hannides, A.K., Krgüer, M. &
- 1059 Boetius, A. (2009). Biogeochemistry of a deep-sea whale fall: Sulfate reduction, sulfide efflux
- 1060 and methanogenesis. *Marine Ecology Progress Series*. 382. pp. 1–21.
- 1061 Welschmeyer, N.A. (1994). Fluorometric analysis of chlorophyll a in the presence of chlorophyll b and
- 1062 pheopigments. *Limnology and Oceanography*. 39 (8). pp. 1985–1992.
- 1063 Wever, T.F., Abegg, F., Fiedler, H.M., Fechner, G. & Stender, I.H. (1998). Shallow gas in the muddy
- 1064 sediments of Eckernförde Bay, Germany. *Continental Shelf Research*. 18. pp. 1715–1739.



- 1065 Wever, T.F. & Fiedler, H.M. (1995). Variability of acoustic turbidity in Eckernförde Bay (southwest
1066 Baltic Sea) related to the annual temperature cycle. *Marine Geology*. 125. pp. 21–27.
- 1067 Whiticar, M.J. (2002). Diagenetic relationships of methanogenesis, nutrients, acoustic turbidity,
1068 pockmarks and freshwater seepages in Eckernförde Bay. *Marine Geology*. 182. pp. 29–53.
- 1069 Widdel, F. & Bak, F. (1992). Gram-Negative Mesophilic Sulfate-Reducing Bacteria. In: A. Balows, H. G.
1070 Trüper, M. Dworkin, W. Harder, & K.-H. Schleifer (eds.). *The Prokaryotes*. New York, NY:
1071 Springer New York, pp. 3352–3378.
- 1072 Wuebbles, D.J. & Hayhoe, K. (2002). Atmospheric methane and global change. *Earth-Science Reviews*.
1073 57 (3–4). pp. 177–210.
- 1074 Zinder, S.H. (1993). Physiological ecology of methanogens. In: J. G. Ferry (ed.). *Methanogenesis*. New
1075 York, NY: Chapman & Hall, pp. 128–206.
- 1076



1077 **Figure Captions**

1078 **Figure 1:** Parameters measured in the water column and sediment at each sampling month in the
 1079 year 2013. Net methanogenesis (MG) and hydrogenotrophic (hydr.) methanogenesis rates are shown
 1080 in triplicates with mean (solid line).

1081 **Figure 2:** Parameters measured in the water column and sediment at each sampling month in the
 1082 year 2014. Net methanogenesis (MG) and hydrogenotrophic (hydr.) methanogenesis rates are shown
 1083 in triplicates with mean (solid line).

1084 **Figure 3:** Parameters measured in the sediment in the gravity core in September 2013.
 1085 Hydrogenotrophic (hydr.) methanogenesis rates are shown in triplicates with mean (solid line).

1086 **Figure 4:** Integrated net methanogenesis (MG) rates and hydrogenotrophic MG rates (0-25 cmbsf) for
 1087 each time point.

1088 **Figure 5:** Potential methanogenesis rates of the four different treatments in November 2013, March
 1089 2014, June 2014 and September 2014. Control (blue symbols) is describing the treatment with
 1090 sediment plus artificial seawater containing natural salinity (24 PSU) and sulfate concentrations (17
 1091 mM), molybdate (green symbols) is the treatment with addition of molybdate (22 mM), BES (purple
 1092 symbols) is the treatment with 60 mM BES addition, and methanol (red symbols) is the treatment
 1093 with addition of 10 mM methanol. Shown are triplicates per depth interval and the mean as a solid
 1094 line. Please note the different x-axis for the methanol treatment (red).

1095 **Figure 6:** Concentrations (A) and isotope composition (B) of porewater methanol (CH_3OH), headspace
 1096 methane (CH_4), and headspace carbon dioxide (CO_2) during the sediment-slurry experiment (with
 1097 sediment from the 0-1 cmbsf horizon in September 2014) with addition of ^{13}C -enriched methanol
 1098 ($^{13}\text{C}:^{12}\text{C} = 1:1000$). Experiment was conducted over 37 days at in-situ temperature (13°C). Shown are
 1099 means (from triplicates) with standard deviation.

1100 **Figure 7:** Sediment methane concentrations over time in the treatment with addition of methanol
 1101 (10 mM) are shown above. Shown are triplicate values per measurement. DNA copies of *Archaea*,
 1102 *Methanosarcinales* and *Methanosarcinaceae* are shown below in duplicates per measurement.
 1103 Please note the secondary y-axis for *Methanosarcinales* and *Methanosarcinaceae*. More data are
 1104 available for methane (determined in the gas headspace) than from DNA samples (taken from the
 1105 sediment) as sample volume for molecular analyzes was limited.

1106 **Figure 8:** Temporal development of integrated net surface methanogenesis (0-5 cmbsf) in the
 1107 sediment and chlorophyll (green) and methane concentrations (orange) in the bottom water (25 m).



1108 Methanogenesis (MG) rates and methane concentrations are shown in means (from triplicates) with
 1109 standard deviation.

1110 **Figure 9:** Principle component analysis (PCA) from three different angles of integrated surface
 1111 methanogenesis (0-5 cmbsf) and surface particulate organic carbon averaged over 0-5 cmbsf (surface
 1112 sediment POC), surface C/N ratio averaged over 0-5 cmbsf (surface sediment C/N), bottom water
 1113 salinity, bottom water temperature (T), bottom water methane (CH₄), bottom water oxygen (O₂), and
 1114 bottom water chlorophyll. Data were transformed into ranks before analysis. a) Correlation biplot of
 1115 principle components 1 and 2, b) correlation biplot of principle components 1 and 3, c) correlation
 1116 biplot of principle components 2 and 3. Correlation biplots are shown in a multidimensional space
 1117 with parameters shown as green lines and samples shown as black dots. Parameters pointing into
 1118 the same direction are positively related; parameters pointing in the opposite direction are
 1119 negatively related.

1120

1121 **Figure 10:** Principle component analysis (PCA) from two different angles of surface methanogenesis
 1122 depth profiles and sampling month (Month), sediment depth, depth profiles of particulate organic
 1123 carbon (POC) and C/N ratio (C/N). Data was transformed into ranks before analysis. a) Correlation
 1124 biplot of principle components 1 and 2, b) correlation biplot of principle components 1 and 3.
 1125 Correlation biplots are shown in a multidimensional space with parameters shown as green lines and
 1126 samples shown as black dots. Parameters pointing into the same direction are positively related;
 1127 parameters pointing in the opposite direction are negatively related.

1128

1129

1130

1131

1132

1133

1134



1135

1136 **Table 1:** Sampling months with bottom water (~ 2 m above seafloor) temperature (Temp.), dissolved
 1137 oxygen (O₂) and dissolved methane (CH₄) concentration

Sampling Month	Date	Instrument	Temp. (°C)	O ₂ (μM)	CH ₄ (nM)	Type of Analysis
March 2013	13.03.2013	CTD	3	340	30	WC
		MUC				All
Juni 2013	27.06.2013	CTD	6	94	125	WC
		MUC				All
September 2013	25.09.2013	CTD	10	bdl	262*	WC
		MUC				All
		GC				GC-All
November 2013	08.11.2013	CTD	12	163	13	WC
		MUC				All
March 2014	13.03.2014	CTD	4	209	41*	WC
		MUC				All
June 2014	08.06.2014	CTD	7	47	61	WC
		MUC				All
September 2014	17.09.2014	CTD	13	bdl	234	WC
		MUC				All

1138 MUC = multicorer, GC= gravity corer, CTD = CTD/Rosette, bdl= below detection limit (5μM), All = methane gas
 1139 analysis, porewater analysis, sediment geochemistry, net methanogenesis analysis, hydrogenotrophic
 1140 methanogenesis analysis, GC-All= analysis for gravity cores including methane gas analysis, porewater analysis,
 1141 sediment geochemistry, hydrogenotrophic methanogenesis analysis, WC= Water column analyses including
 1142 methane analysis, chlorophyll analysis

1143 **Concentrations from the regular monthly Boknis Eck sampling cruises on 24.09.13 and 05.03. 14 (www.bokniseck.de)

1144

1145

1146

1147

1148

1149

1150

1151



1152 **Table 2:** Comparison of surface methanogenesis rates in shallow water marine sediments of different
 1153 geographical origin

Study site	Water depth (m)	Sediment depths (cm)	Rate (nmol cm ⁻³ d ⁻¹)	Reference
<i>Sulfate-containing, organic-rich sediments</i>				
Eckernförde Bay (Baltic Sea)	28	0-25	0-1.3	Present study
Upwelling region off Peru (Pacific)	70-1025	0-25	0-1.5	(Maltby et al., 2016)
Upwelling region off Chile (Pacific)	87	0-6	0-0.6	(Ferdelman et al., 1997)
Limfjorden (North Sea)	7-10	0-100	0-0.05	(Jørgensen & Parkes, 2010)
Colne Point Saltmarsh (Essex, UK)	-	0-30	0-0.03	(Senior et al., 1982)
<i>Sulfate-depleted, organic-rich sediments (sediment depth marks the depth at which sulfate was depleted)</i>				
Eckernförde Bay (Baltic Sea)	28	> 100	0.01-1.4	Present Study
Limfjorden (North Sea)	7-10	> 100	0.01-3.1	(Jørgensen & Parkes, 2010)
Saanich Inlet (British Columbia, Canada)	225	> 20	0.3-7.0	(Kuivila et al., 1990)
Upwelling region off Peru (Pacific)	78	> 50	0-2.1	(Maltby et al., 2016)

1154

1155

1156

1157

1158

1159

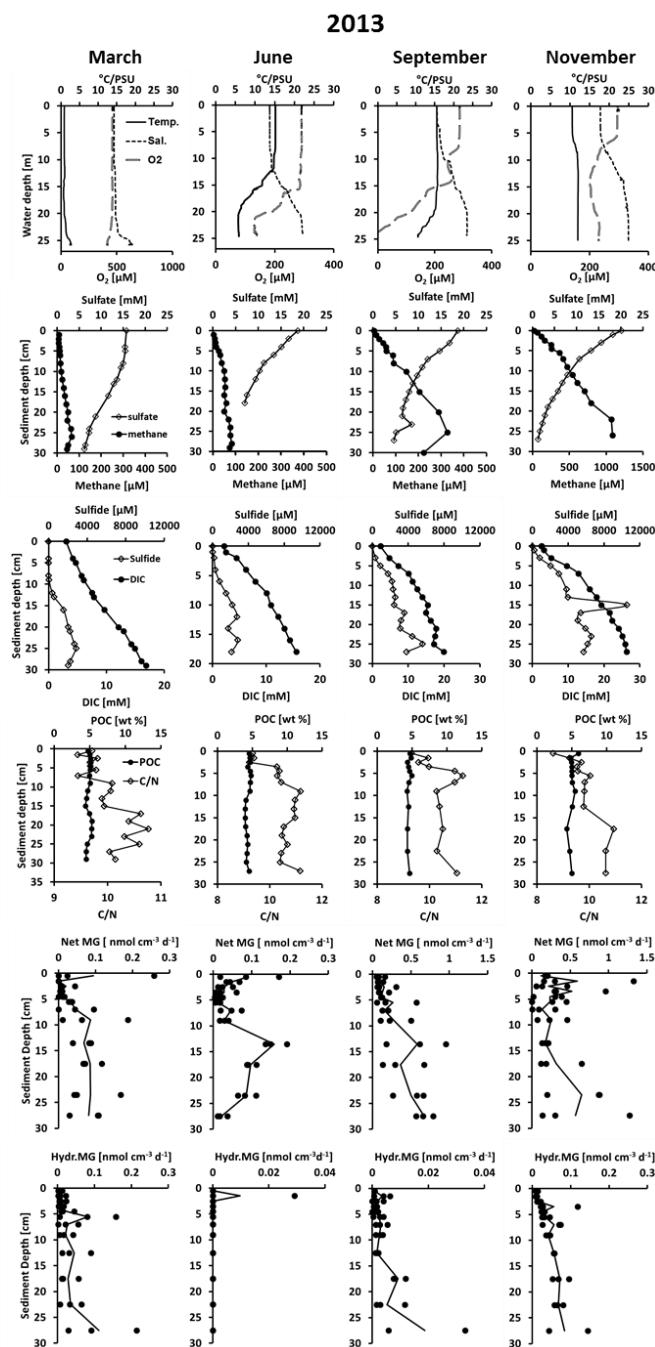
1160

1161



1162 Figures

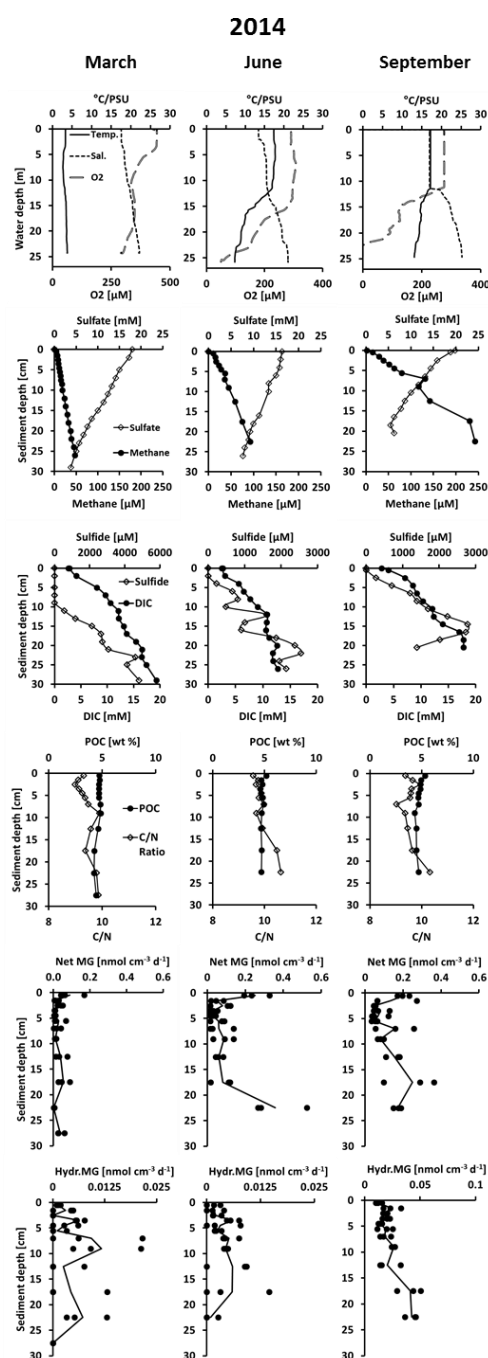
1163 Figure 1



1164



1165 **Figure 2**



1166

1167



Figure 3

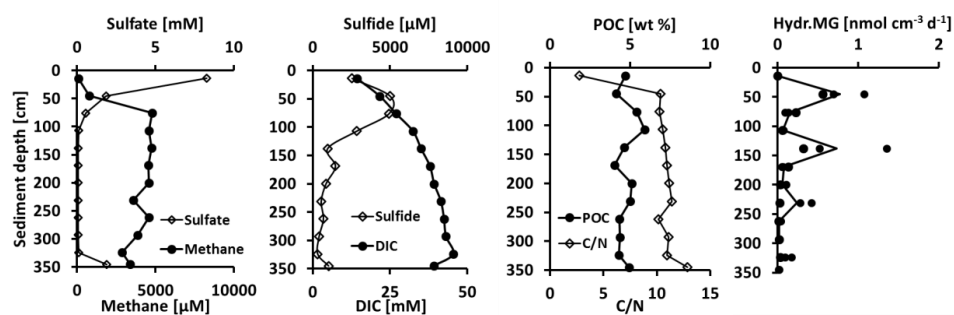




Figure 4

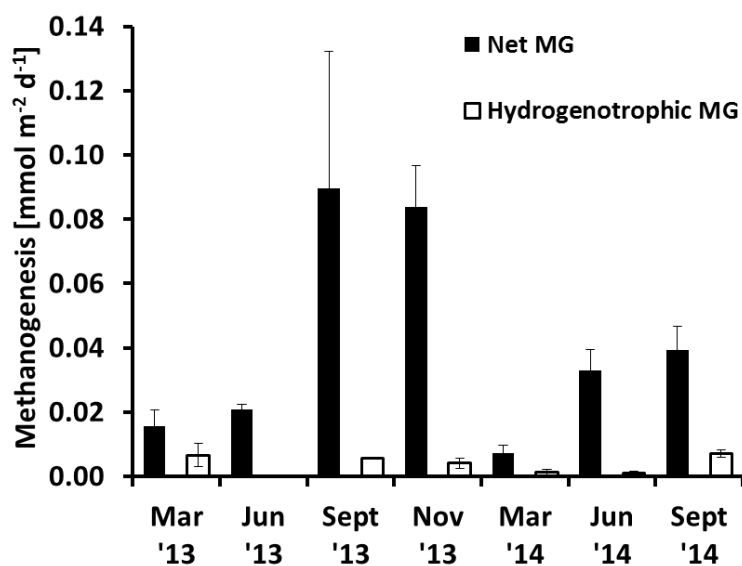
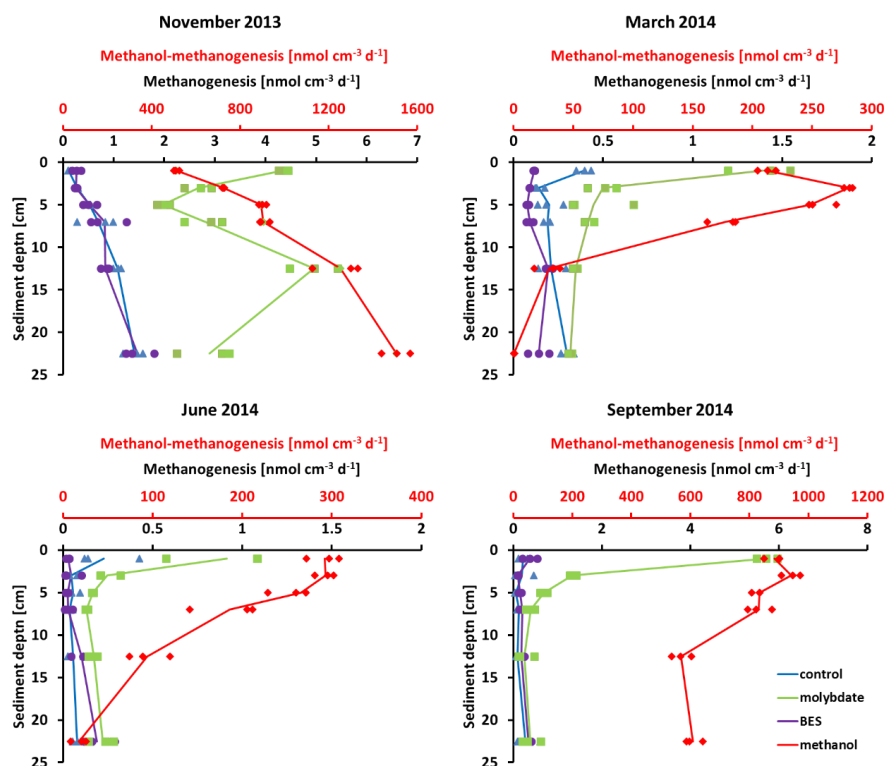


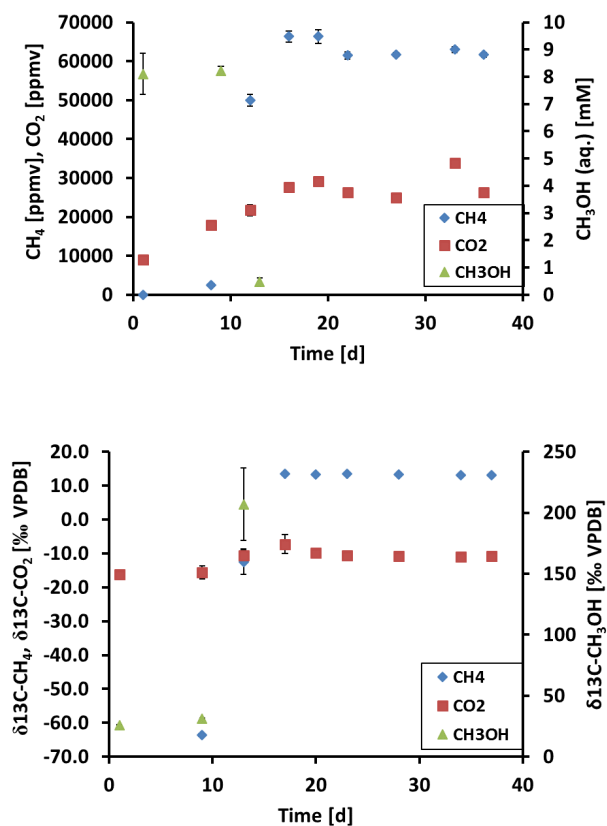


Figure 5





1214 **Figure 6**



1215

1216

1217

1218

1219

1220

1221

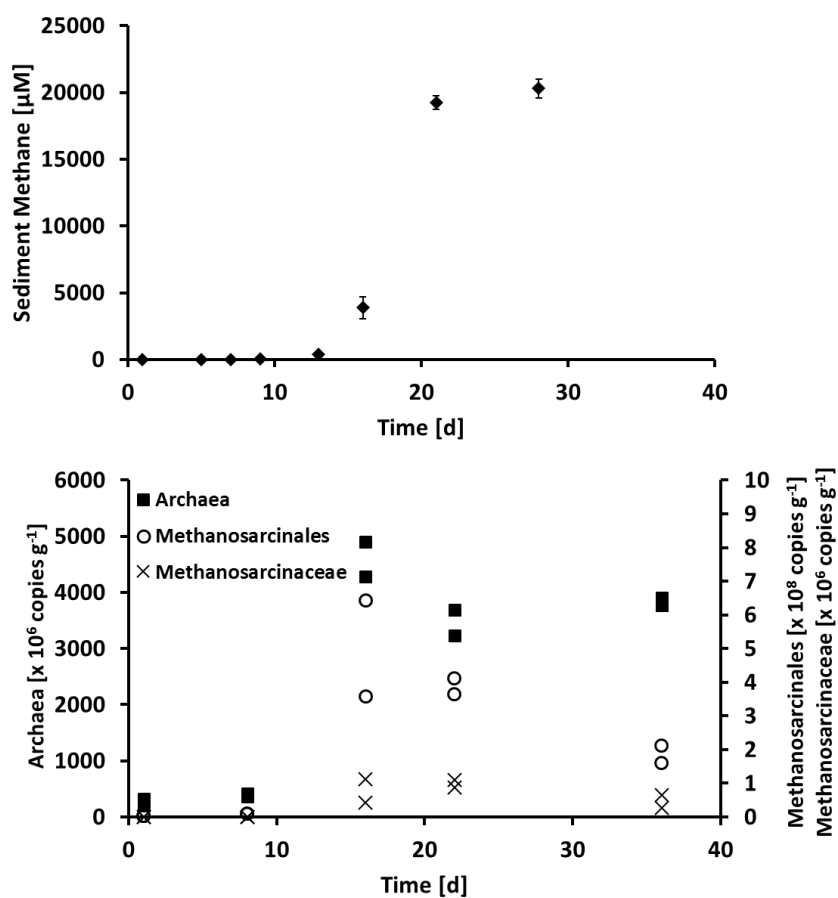
1222

1223

1224



1225 **Figure 7**



1226

1227

1228

1229

1230

1231

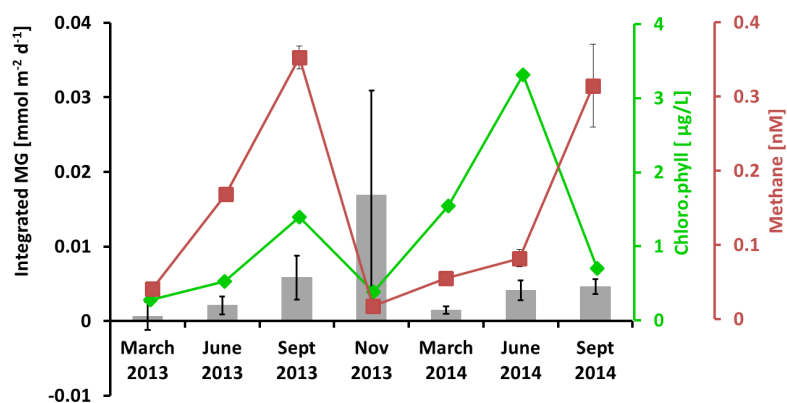
1232

1233

1234

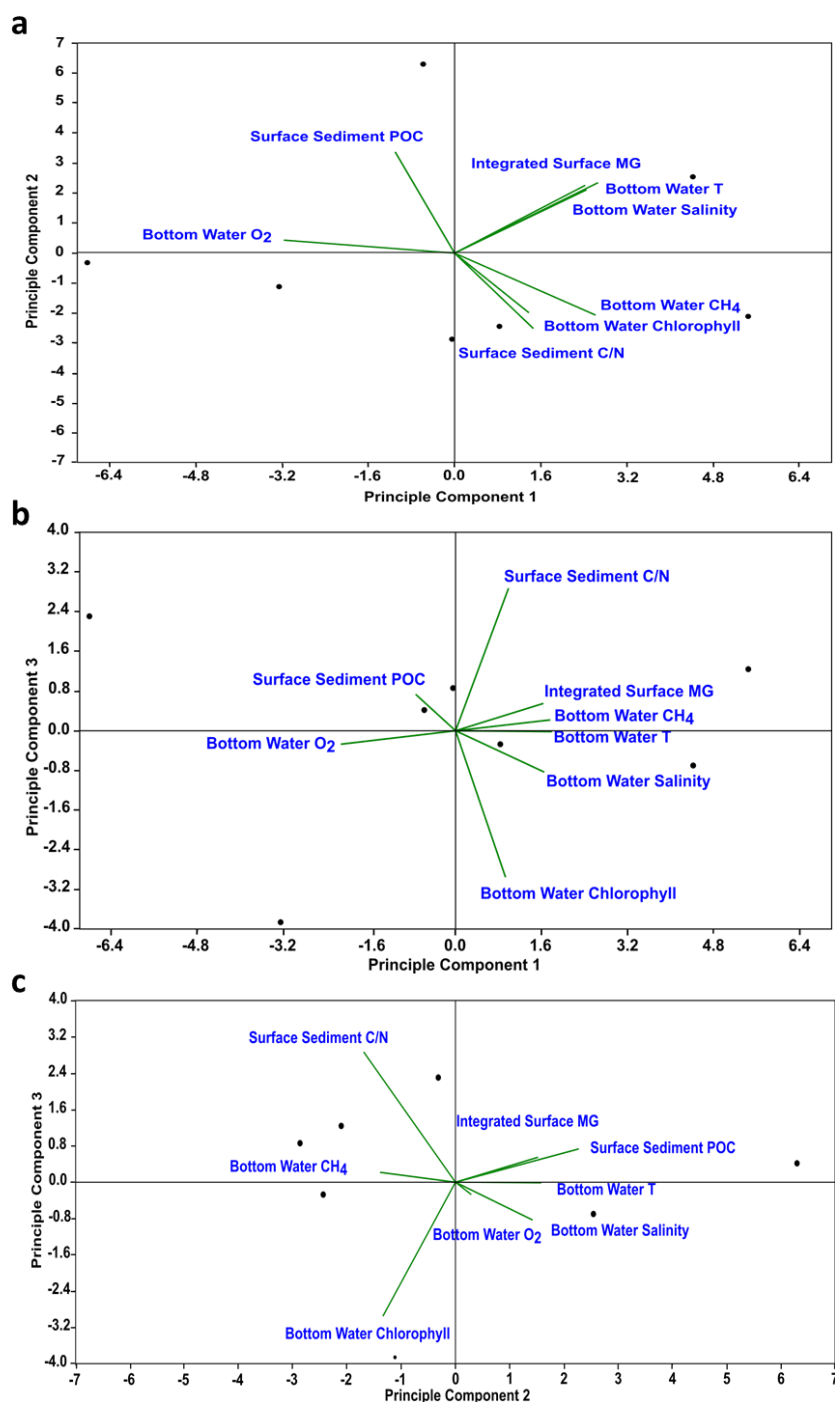


1235 **Figure 8**





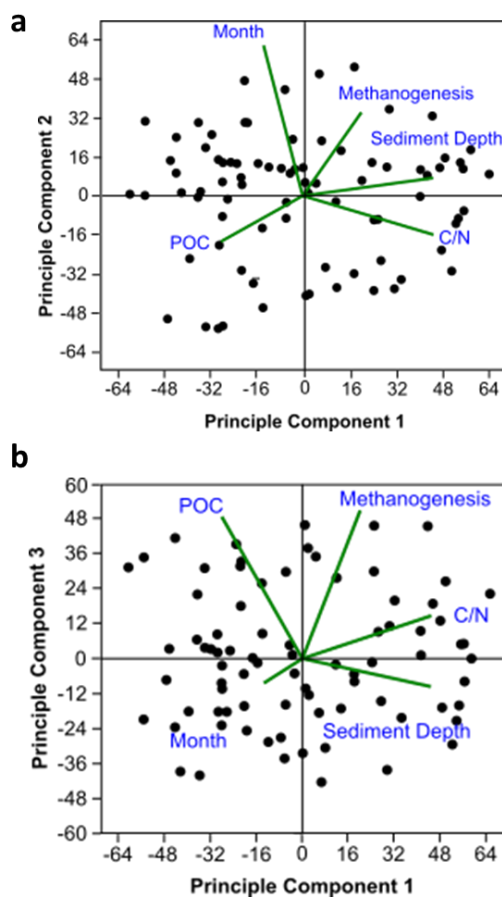
1251 **Figure 9**



1252



1253 **Figure 10**



1254

1255

1256

1257

1258

1259

1260

1261